arXiv:astro-ph/0304255v3 11 Aug 2003

Matching the Cosmic Star Formation History to the Local Galaxy Population

Neil Trentham
Institute of Astronomy
University of Cambridge
Madingley Road
Cambridge CB3 0HA
United Kingdom

ABSTRACT

In this review I will describe a number of recent advances in extragalactic astronomy. First of all I will describe our current best estimates of the star formation history of the Universe. Then I will describe measurements of local galaxies and their stellar populations, concentrating on measurements of the luminosity functions and stellar population compositions of the different kinds of galaxies. Finally, I will investigate the relationship between these two sets of results. The ultimate aim is to tell at what stage in the history of the Universe the different stars seen in the local galaxies formed. At present much is known but there are significant uncertainties and I will highlight some prospects for the future.

1 INTRODUCTION

Extragalactic astronomy is a particularly active area of scientific research. Of particular importance is the recognition that the formation and evolution of galaxies are essentially *cosmological* processes and that extragalactic astronomy is intimately related to cosmology.

There are essentially two kinds of matter in galaxies: dark matter and luminous matter. The dark matter is probably cold, meaning that it does not diffuse out of gravitational condensations [1,2]. Its formation is tied up with the physics of the early Universe and its assembly into discrete galaxies is caused by the gravitational growth of small perturbations present at very early times [3]. Most luminous matter is in the form of stars, and it is the distribution of these stars into populations in different kinds of galaxies and the formation of these stellar populations that is the subject of this review.

One area of study of considerable current interest is the determination of the star-formation history of the Universe i.e. determining when in the past the stars seen now in galaxies formed. Classically, this was determined from optical surveys of field galaxies [4]. But we know that the far-infrared background measured by *COBE* [5,6,7] is high, suggesting that much of cosmic star-formation could be dust-enshrouded and missing from optical surveys. Submillimetre surveys (e. g. ref. 8) then confirmed a great deal of star-formation was indeed happening in infrared galaxies that are optically faint. These are separate galaxies from those seen in optical surveys, so we are not talking about large amounts of obscured star formation happening within optically-identified galaxies of known redshift, rather a new population of galaxies altogether. The submillimetre surveys showed that the galaxies exist in enough number to explain the far-infrared background and possibly dominate the cosmic star-formation history. Unfortunately the large beamsize of the SCUBA instrument used in these surveys means that we cannot identify the infrared galaxies individually so that we cannot study them and determine their redshifts. In an important recent development [9,10,11], four such infrared galaxies have been identified by virtue of hosting gamma-ray bursts (a phenomenon which seems to be intimately linked with ongoing star formation). These four galaxies are exactly what we expected them to be: the have high (> 100 $M_\odot$ yr^{-1}) star-formation rates inferred from submillimetre and/or optical measurements, but low optical fluxes, presumably due to internal obscuration. So while we are still some way from determining the redshift distribution of these infrared galaxies (only four are known), we are now beginning to compile a sample which can be studied in some detail.

The accurate determination of the galaxy luminosity function $\phi(L)$, defined as the number density of galaxies per unit luminosity L, has been another active area of study. The general form of the total galaxy luminosity function is well described by the Schechter function [12]:

$$\phi(L) = \phi^* \exp(-\frac{L}{L^*}) \left(\frac{L}{L^*}\right)^{\alpha} \frac{1}{L^*}, \quad (1)$$

where ϕ^* is a characteristic density, L^* is a characteristic luminosity, and α is the faint-end slope. This function provides an acceptable fit to the total galaxy luminosity function in both clusters and the field, although the contributions to the total luminosity function from different galaxy types is somewhat different in the two environments (e.g. ref. 13): in clusters ellipticals and lenticulars dominate at the bright end and dwarf ellipticals at the faint end whereas in the field spirals dominate at the bright end and dwarf irregulars and dwarf ellipticals exist in equal number at the faint end.

Two lines of current research have been relevant in this context. Firstly, the normalization of the galaxy luminosity function, and consequently the luminosity density of the Universe, has been determined from large redshift surveys like SDSS [14] and 2dF (see ref. 15, where this redshift survey is considered in conjunction with the 2MASS near-infrared survey). Secondly, the contribution from galaxies with extremely low surface brightnesses has been shown to be small, from deep optical surveys (e. g. ref. 16).

It has been conventional to assume that almost all the gas which was converted into stars within galaxies exists in the stellar populations that we see today. The possibily that this view may be incorrect has recently been suggested by the result of the MACHO gravitational microlensing project [17]: as much as a few percent of galactic halos may be made up of objects with masses of about 0.5 $M_\odot$. Two possibilities are that these are stellar remnants like cold white dwarfs [18; however see ref. 19] or low-mass stars that failed to initiate nuclear burning for some reason. Either of these scenarios would require that most of the star formation that happened over the history of the Universe occurred in galaxy *halos*, which is very much in contradiction to the traditional view.

In this article we review both measurements of the cosmic star formation history and of the distribution of stars in galaxies in the local Universe. We then review the techiques that can be employed to match the two sets of observations so that we know at what point in the history of the Universe the stars that we see in the galaxies around us formed. Prospects for the future are highlighted. While we will concentrate on the traditional view that most stars formed in high-density environments well inside dark-matter halos and all but the highest-mass ones (whose lifetime plus the age of the Universe at the redshift of formation is less than a Hubble time) exist in the visible parts of galaxies today, we will also discuss the implications of the assertions outlined in the previous paragraph.

Earlier it was remarked that extragalactic astronomy is closely related to cosmology, and consequently the values of many quantities depend on the cosmological model chosen. Masses derived from gravitational motions are proportional to the luminosity distance d_L and luminosities derived from fluxes scale as d_L^2. Number densities scale as V^{-1} so mass densities scale as $d_L V^{-1}$ and luminosity densities as $d_L^2 V^{-1}$, where V is the cosmological volume element. The star-formation rate density at any redshift z is usually derived from a luminosity density and similarly depends on $d_L(z)^2 V(z)^{-1}$; for a given cosmological model the star-formation rate density is therefore proportional to the Hubble constant h since $d_L \propto h^{-1}$ and $V \propto h^{-3}$. The current density in stars ρ_* is proportional to the-integral of this star-formation rate density and so independent of h (and is weakly dependent on the cosmology). Expressed in units of the critical density $\Omega_* = \rho_*/\rho_c$, then $\Omega_* \sim h^{-2}$, since $\rho_c = 3H_0^2/8\,\pi G \sim h^2$. These sscaling relations assume that the luminosity-to-star-formation-rate conversion factor (this comes from a Galactic calibration) does not depend on the Hubble constant.

Stellar densities derived from the local luminosity function do not depend on the cosmology and have a different dependence on the Hubble constant. Luminosities scale as h^{-2} and volumes as h^{-3} so that the luminosity density of the Universe scales as h. Therefore $\rho_* \sim h$ and $\Omega_* \sim h^{-1}$. The above scaling relations assume that the stellar mass-to-light ratios of galaxies (normally these come from population synthesis models) do not depend on the Hubble constant.

Throughout this work we will assume a model with a non-zero cosmological constant: $h = 0.65$ (h is the Hubble constant H_0 in units of 100 km s^{-1} Mpc^{-1}), $\Omega_\Lambda = 0.7$, $\Omega_{\rm matter} = 0.3$. The luminosity-distance for this model [20] is $d_L(z) = \frac{c}{H_0}\,(1+z)\,\int_0^z \frac{1}{\sqrt{(1+z')^2(1+\Omega_{\rm matter}z') - z'(2+z')\Omega_\Lambda}}\,{\rm d}z'$.

2 THE COSMIC STAR FORMATION HISTORY

2.1 The Madau Plot

The star formation history of the Universe is normally presented as the "Madau" or "Madau-Lilly" Plot [4,21]. The ordinate axis of this plot is redshift z, which is related directly to cosmic time, assuming some cosmological model (see Table 1, which is appropriate for a model with a cosmological constant; e.g. ref. 22). The abscissa axis of this plot is the total star-formation rate happening within some average volume element that is comoving with the Hubble flow. At the present time ($z = 0$) this volume element represents some typical Mpc^3 in the Local Universe.

Most contemporary observations suggest that the Madau Plot is best considered in two parts–an optical part and an infrared part. The optical part is very well determined from a large number of redshift surveys currently being performed with large telescopes (see ref. 23 for a compilation). The idea here is to construct an (optical) flux-limited sample of galaxies and measure redshifts for those galaxies.

Table 1

Age of Universe for $h = 0.65$, $\Omega_\Lambda = 0.7$, $\Omega_{\rm matter} = 0.3$ cosmology*

Redshift z	Age/Gyr
0	14.5
1	6.2
2	3.5
3	2.3
4	1.6
5	1.2
10	0.5

*Note that age $t(z) = \frac{c}{H_0} \int_z^\infty \frac{1}{1+z'} \frac{1}{\sqrt{(1+z')^2(1+\Omega_{\rm matter} z') - z'(2+z')\Omega_\Lambda}} {\rm d}z'$ [ref. 20].

The infrared part is less well-determined. The galaxies that are important here are those whose optical and ultraviolet light, which comes from young OB stars and traces ongoing star formation directly, has been extinguished by dust. This dust is made of graphite and silicates produced within the star-forming galaxies in red giant atmospheres and supernovae [24]. These galaxies are faint at optical wavelengths and are consequently missing from the redshift surveys described above. Even if the *galaxy* is present in optical surveys due to some residual optical light that escapes or is generated at low skin-depth, the vast majority of the star formation is unaccounted for if optical observations alone are available. We know that large numbers of these infrared galaxies exist from the high infrared background [5,6,7] and from submillimetre galaxy surveys (ref. 25 and references therein), but the galaxies cannot generally be identified on an individual basis so that we cannot determine their redshifts and therefore we cannot place them on the Madau Plot.

What is becoming increasingly clear is that the populations of optical and infrared galaxies that contribute to the two parts of the Madau Plot are basically disjoint. This statement is not 100% true, but provides a useful starting position to adopt. Infrared galaxies have low optical fluxes due to internal dust obscuration and optical galaxies, like high-redshift Lyman-break galaxies, tend to have low infrared and submillimetre fluxes [26] because their total star formation rates and energy outputs tend to be small in comparison with infrared galaxies. A small number of galaxies exist which have extremely high infrared *and* optical luminosities (the "Class-2" sources of Smail et al.[25], but these are rare. They can, however, be studied in detail by virtue of their optical identification - the prototype is SMM J02399−0136 [27].

It is worth explaining in this context exactly what is meant by "infrared" as opposed to "optical" galaxy. The important discriminant is whether or not a reasonable fraction (say 50% or so) of the star formation in a galaxy can be inferred from optical observations. Most "optical" galaxies, like the Milky Way and late-type spiral galaxies, emit much of their energy at far-infrared wavelengths so that much of the star formation accounted for in the "optical" part of the Madau Plot includes a contribution from star formation absorbed and reradiated by dust. But the crucial thing to note in this context is that these galaxies also emit a reasonable proportion of their energy at rest-frame optical and ultraviolet wavelengths (see Figure 2 of ref. 28). "Infrared" galaxies do not do this and we only have a realistic measure of their energy output and star-formation rate from far-infrared/submillimetre (or radio continuum) observations. We will see that a good prototype of an "infrared" galaxy is the host galaxy of GRB 980703, where the optically-derived star formation rate is 10 – 30 $M_\odot$ yr^{-1} [29] but the total (infrared + optical) star formation rate is more like 500 $M_\odot$ yr^{-1} [9]. The fraction of the star-formation in this galaxy determined by optical measurements is therefore only 4%, much less than the 30 – 70% that is typical for local late-type star-forming galaxies [28].

The two types of star-forming galaxies could well have different redshift distributions. We cannot therefore obtain the infrared Madau Plot simply by multaplicative scaling of the optical Madau Plot.

The proportion of the total star formation happening in the Universe in infrared galaxies $f_{\rm IR}$ is probably greater than 50% [30]. One plausible scenario consistent with current observation is presented in Figure 1. The optical

Madau plot, as indicated by the dashed line, is very well determined by a large number of observations (the filled circles) but the infrared part (the solid line minus the dashed line) is poorly constrained and is model-dependant, and we only really know its integral over redshift (and even then with considerable uncertainty).

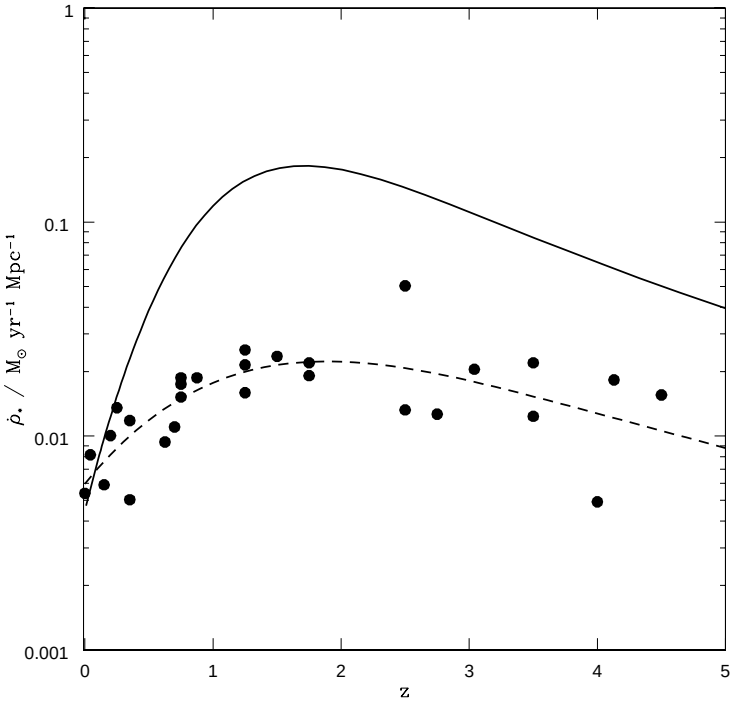

Figure 1: The comoving star-formation rate of the Universe as a function of redshift, from ref. 30. The points represent the optical data compiled by Somerville et al. (ref. 23) with no corrections for dust extinction; the dashed line represents a 4th-order polynomial fit to this data – the optical Madau plot. The solid line represents an estimate of the total (optical and infrared) Madau plot, from the models of Blain [31,32,33], assuming no AGN contribution to the far-infrared and submillimetre backgrounds and counts. The stellar IMF of Kroupa, Tout & Gilmore [34] is assumed.

2.2 The Extragalactic Background Light

The extragalactic background radiation emerging at different wavelengths is shown in Figure 2. The total extragalactic background light (EBL) is given by the integral over wavelength of the line in Figure 2 and is approximately equal to 55 nW m^{-2} sr^{-1} (ref. 35).

The EBL shows two peaks: an optical/near-infrared one at about 1 μm and a far-infrared one at about 100 μm. The optical-near-infrared EBL is derived by summing galaxy counts from field surveys [35,36]. The far-infrared background comes from *COBE* DIRBE [5,6] and FIRAS [7] measurements.

The total energy in the optical regime of the EBL is approximately equal to the total energy in the far-infrared regimes. A useful exercise is to attempt to translate this observation into a value of $f_{\rm IR}$. In order to do this we need to consider two further issues.

Firstly, we must establish which parts of the EBL come from physical processes other than star formation. Radiation from old, evolved, stars is certainly a contributor to the EBL, but this radiation is unlikely to be mistaken for radiation originating from young newly-formed OB stars since old stars have spectral energy distributions (SEDs) peaked in the near-infrared, whereas young stars have SEDs peaked at optical or ultraviolet wavelenghs and any enshrouding dust has an SED peaked at far-infrared wavelengths. The contribution from active galactic nuclei (AGNs) is potentially more difficult to correct for, since these (and their associated dust shrouds) can in principle radiate energy at any wavelength. Indeed, if quasars form via the evolutionary sequence [37,38] cold

ultraluminous infrared galaxy (ULIG; e.g. Arp 220) → warm ULIG (e. g. Markarian 231) → infrared quasar (e. g. I Zw 1) → optical quasar (e. g. 3C 273; these could be radio-loud late in their evolution), then we might expect AGNs to contribute at some level to both the far-infrared (when they are cold ULIGs) and optical (when they are quasars) backgrounds. However, we do not expect the contribution to the EBL from AGNs to be large, else the local density of supermassive black holes in the centers of nearby galaxies, the end products of AGN activity, would be larger than that observed [39]. The total contribution to the EBL from AGNs (assumed to happen at mean redshift $< z_{\rm AGN} >$ and efficiency η, which is 0.057 for disk accretion onto a Schwarzchild black hole) is $I_{\rm AGN} = 5 \left(\frac{h}{0.65}\right) \left(\frac{\eta}{0.057}\right) \left(\frac{3}{1+<z_{\rm AGN}>}\right)$ nW m^{-2} sr^{-1}, which is about 10% of the total EBL [35]. This turns out to be smaller than the other uncertainties, like those described in the next paragraph.

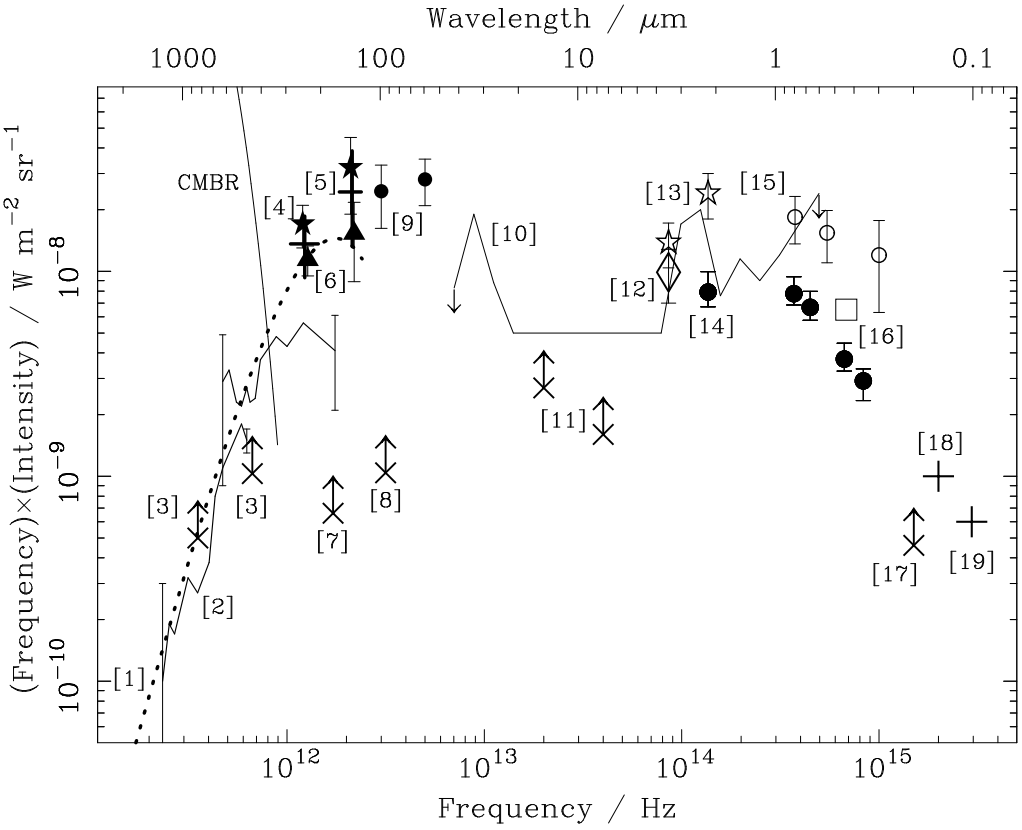

Figure 2: The extragalactic background light, from ref. 40. This figure was compiled using many literature sources, represented by the numbers. The reader is referred to ref. 40 for the original sources. The cosmic microwave background radiation spectrum is also shown.

Secondly, the average redshifts of the galaxies that contribute to the optical and infrared parts of the Madau Plot may be different. The extragalactic background intensity $I_* \propto \dot{\rho_*} (1+ < z >)^{-1}$, where $< z >$ is the mean redshift of the sources (assumed to form stars at an average rate $\dot{\rho_*}$) contributing to I. Consequently if the infrared sources are at significantly higher redshift than the optical ones, then they may trace the formation of a larger mass of stars for a given amount of background radiation generated.

We can now estimate $f_{\rm IR}$ from the extragalactic background light as follows. In addition to the simplifications described in Section 2.1, let us consider approximating the background radiation by two parts (representing the two regimes in Figure 2): an optical part $I_{\rm opt}$ and an infrared part $I_{\rm IR}$. Let us assume that the infrared galaxies are at an average redshift $< z_{\rm IR} >$ and that the optical galaxies are at an average redshift $< z_{\rm opt} >$ and further that the optical galaxies emit an average fraction R of their energy in the infrared ($R \sim 0.5$ for local galaxies [28] but might be significantly different at higher redshifts). Then all other things (like the stellar initial mass function

and the bolometric-luminosity to star-formation-rate conversion factor) being equal,

$$f_{\rm IR} = \frac{1}{1 + \frac{(1+<z_{\rm opt}>)}{(1+<z_{\rm IR}>)} \left((1-R) \frac{I_{\rm IR}}{I_{\rm opt}} - R \right)^{-1}}. \quad (2)$$

Although there are many assumptions inherent in applying this equation it is useful to note the important result: the greater $< z_{\rm IR} >$ for a given $< z_{\rm opt} >$, the higher $f_{\rm IR}$ for a given ratio of $I_{\rm IR}$ and $I_{\rm opt}$.

2.3 The Optical Madau Plot

For an optically-selected sample of galaxies, if redshifts and distances are available for all the galaxies, then if we are able to estimate star-formation rates for the galaxies from ultraviolet or Hα luminosities, we can place them on the Madau Plot. For any complete sample, the optical Madau Plot can then be derived. This completeness has to be present both in terms of

(i) luminosity: this is achieved if the faintest galaxies in the sample have low enough luminosity and are far enough down the Schechter (1976) luminosity function that the total luminosity density in fainter galaxies is small; if this is not true then a correction to the cosmic star formation rate can be made to take into account the contribution from these low-luminosity galaxies, assuming that star-formation rate scales with luminosity;

(ii) surface-brightness: galaxies with surface-brightnesses significantly below the sky will be missing from optically-selected samples, but corrections due to this effect are normally assumed negligible since the fraction of the luminosity density in low-surface-brightness star-forming galaxies is small.

At low redshifts $z < 1$ spectroscopic redshifts may be obtained for optically complete (in a flux-limited sense) samples and the cosmic star formation rate derived from measurements of the Hα 656.3 nm [41,42] or [OII] 372.7 nm [43,44] lines. The cosmic star formation rate at low z is presented in those papers (see also ref. 45). For redshifts $1 < z < 3$ it is not practical to obtain spectroscopic redshifts for complete samples so that photometric redshifts (e.g. ref. 46) are often used (the deepest surveys, like the Caltech Faint Galaxy Redshift Survey are highly complete only to $z \sim 1.5$ [47]). Additionally, for $z > 1$, the Hα line is redshifted from the optical to the near-infrared, so that Hα luminosities are difficult to obtain for complete samples – ultraviolet/optical luminosities then become the most direct method of estimating star formation rates. At higher redshifts $3 < z < 5$ galaxies can be selected from optical surveys using the Lyman-break technique [48]. Spectroscopic redshifts can then be obtained for these Lyman-break galaxies and star-formation rates derived from their rest-frame ultraviolet luminosities. The optical Madau Plot at $3 < z < 5$ can then be constructed from the samples of Lyman-break galaxies [49].

Much of the energy produced by young OB stars in these optical galaxies is absorbed by dust and reradiated at far-infrared wavelengths (the SED of many optical galaxies has a peak in the far-infrared). This is what we parameterized by the variable R in the previous paragraph. Each measured point on the optical Madau Plot must be therefore multiplied by a factor $P \approx (1-R)^{-1}$. The value of P depends on the redshift and on the nature of the tracer used to derive the star formation rate. At $z \sim 0$, the star-formation tracer is the Hα (656.3 nm) luminosity and $P \sim 2$ (ref. 28). An interesting estimate of P is provided by ISO mid-infrared 15 μm observations [50]. This work suggests that $P \sim 3$ at a mean redshift 0.6. At high redshifts $z \sim 4$, the star-formation tracer is the ultraviolet luminosity at about 150 nm, which is very susceptible to attenuation by dust [51,52]. Consequently a higher value of $P \sim 5$ is required [49; however see the discussion in ref. 53 abour the concordance between Hβ and ultraviolet star-formation rates in Lyman-break galaxies].

At very high $z > 5$ we expect the cosmic star formation rate to be dominated by optical, not infrared, galaxies since the Universe has not had enough time to generate the large amounts of dust required to produce infrared galaxies. Break techniques can certainly be used to find $z > 5$ galaxies (e.g. refs. 54 and 55), but at the highest redshifts the most profitable technique is likely to be narrowband imaging searches for Lyα emitters [56]. These high z emission-line searches are helped by the redshift-dependence of equivalent width EW $\sim (1+z)$, and the technique has been successful at finding galaxies up to a redshift $z = 6.56$ [57]. Converting Lyα emitter space densities into a cosmic star formation rate is difficult since it is not possible to establish what fraction of optical galaxies of a given redshift *are* Lyα emitters (above some luminosity threshold). This fraction might be quite low since Lyα is a resonant line and photons may be subject to multiple scatterings and have a low escape fraction; many galaxies with high star-formation rates may have low Lyα luminosities. From measurements of Lyα emitters, Hu et al. [56] estimate a lower limit on the cosmic star formation rate (adapted to our cosmology and stellar IMF

– see Section 1 and Figure 2) of about 0.003 – 0.006 $M_\odot$ yr^{-1} Mpc^{-3} for redshifts $3 < z < 6$, which is less than the value of 0.09 $(P/5)$ $M_\odot$ yr^{-1} Mpc^{-3} measured at $z \sim 4$ from Lyman-break surveys [49]. A somewhat higher range of 0.07 – 1.4 $M_\odot$ yr^{-1} Mpc^{-3} has been estimated at $z = 6.6$ [57].

It is important to note that the only measurable quantity in all the surveys described above is a luminosity density, and that if an appreciable fraction of cosmic star formation happened in environments where this luminosity density is low, much could be missed due to $(1 + z)^{-4}$ cosmological surface-brightness dimming [58]. The determinations of the cosmic star-formation rate at any redshift from these surveys should therefore be regarded as lower limits, more so at the highest redshifts.

2.4 The Infrared Madau Plot

The infrared Madau Plot represents the total star formation so obscured that it is very much under-represented the optical (rest-frame ultraviolet at high redshift) surveys described in the previous section. It is *not* merely the absorbed and reradiated light from optical galaxies (parameterized by P and R); this reradiated energy is not sufficient to explain the high infrared background.

At $z = 0$, ultraluminous infrared galaxies (ULIGs; ref. 59) like Arp 220 are the types of galaxies with these properties – unremarkable at optical wavelengths but very luminous in the infrared. But these contribute negligibly to the global $z = 0$ star-formation rate. Furthermore, were they to exist at high redshift, ULIGs could not have produced the local galaxy population. This is because the molecular gas density in the central regions generating most of the energy in ULIGs is high (> 100 $M_\odot$ pc^{-3}), whereas a negligible fraction ($\sim 1\%$) of the stars in the local Universe – elliptical galaxy centres – exist at such high densities [60]. Semi-analytic models [61] also predict that the gas in galaxies generating the infrared Madau Plot must be somewhat more extended than in local ULIGs. Large reservoirs of extremely dense cold gas at high redshift are certainly known to exist (e. g. around APM 08279+5255 at $z = 3.9$ [62]) so it is quite possible that these exist and are associated with much of the cosmic star formation.

It is interesting to note that the star-formation rate at $z = 0.6$ measured from a 15-μm sample observed with *ISO* [50] corresponds exactly to the star-formation rate determined from optical measurements [21] with $P = 3$. This implies either at $z = 0.6$ infrared galaxies contribute negligibly to the Madau Plot or the dust temperatures in the infrared galaxies are so low that their SEDs peak at long enough wavelengths that their 15-μm fluxes are small. This latter possibility is what is suggested by the submillimetre observations described in the next section.

2.4.1 Constraints from submillimetre surveys

Submillimetre surveys are one way to find high-redshift infrared galaxies. Although submillimetre measurements probe well down the Rayleigh-Jeans long-wavelength tail of the SED of most infrared galaxies, current submillimetre cameras, like the SCUBA bolometer array on the JCMT in Hawaii [63] operating at 850 μm and 450 μm, are only sensitive enough to find the most luminous of these galaxies. The main issue preventing very deep surveys is source confusion [64]. Observing gravitationally lensed sources behind massive galaxy clusters [8] increases the sensitivity of SCUBA by factors equal to the magnifications of the background sources, typically 2 – 5 [25].

The submillimetre number counts are presented in Figure 3. It is immediately obvious from this figure that the submillimetre counts probe to a far deeper equivalent flux limits than *ISO* infrared surveys. The *ISO* surveys probe closer to the SED peaks of the majority of the infrared galaxies but the telescope + detector efficiency is lower.

The exact form of the 850-μm counts is only well constrained at high fluxes. Between 2 mJy and 10 mJy the differential number counts are approximately $n(S) \approx 30000\,(0.7 + S)^{-3.2}$, where S is the flux density in mJy [65]. Fainter than about 1 mJy, the counts are constrained primarily by the extragalactic background light $\int S\,n(S)\,\mathrm{d}S$, which at 850 μm is about 0.55 nW m^{-2} sr^{-1} [7]. Combining these results, Barger et al. [65] show that the bulk of the 850-μm background light comes from sources with fluxes of about 1 mJy and inferred star formation rates of about 200 $M_\odot$ yr^{-1}.

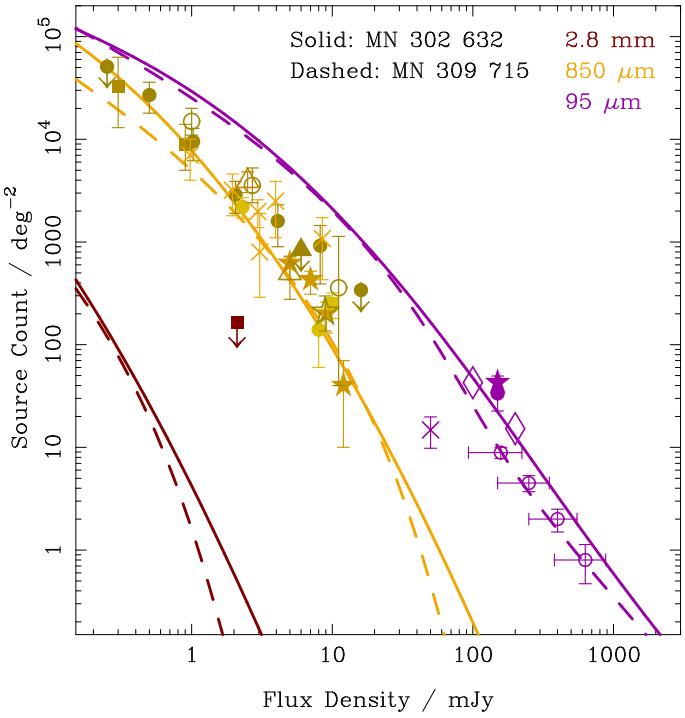

Figure 3: Galaxy number counts in the far-infrared, submillimetre, and millimetre regimes, from ref. 40. The data is compiled from many sources and the reader is referred to ref. 40 for the original sources. The light points represent 850-μm SCUBA counts, the dark points on the right represent 95-μm *ISO* data, and the dark square on the left represents the 2.8-mm BIMA limit of Wilner & Wright [66]. The lines represent two models from the literature.

Aside from verifying the fact that the infrared galaxies exist in the right number to produce the extragalactic background light, the main information to be gained from the submillimetre observations are the luminosities and temperatures of the galaxies. Luminosities (and hence star formation rates) can be obtained from fluxes even if we do not know the redshifts because infrared galaxies have negative K corrections at 850 μm: $f_\nu = L_{\nu(1+z)}(1+z)/4\pi d_L(z)^2$ and infrared galaxies have SEDs where an increase in redshift causes $L_{\nu(1+z)}$ to increase by an amount approximately equal to the increase in $d_L(z)^2/(1+z)$ at 850 μm for $1 < z < 4$. The total luminosity $L = \int_0^\infty L_\nu \mathrm{d}\nu$, where L_ν at any frequency can be derived from its value at 850 μm if the dust temperatures are known. Temperatures are known to be close to 37 K due to joint consideration of 850-μm and 450-μm counts and modeling [32,67]. Further information is difficult to obtain because of the large SCUBA beamsize FWHM $\sim$ 14 arcseconds. Normally we cannot tell which of the large number of optical sources (if any) within the SCUBA beam is the submillimetre source and this lack of optical identification means we cannot obtain the redshift.

A number of submillimetre galaxies do have optical or near-infrared counterparts but these are rare, particularly at the low 850-μm fluxes responsible for generating most of the background. Examples include the Class-2 SCUBA galaxies [25], like SMM J02399−0136 ($z = 2.80$ [27]), SMM J14022+2512 ($z = 2.56$) and SMM J02399−0134 ($z = 1.06$). These are lightly obscured star-forming galaxies with huge optical/UV and Hα star-formation rates, so high that the reradiated energy from the stars that *have* been obscured is enough to make these into luminous submillimetre galaxies. Other examples are extremely red objects (EROs, or Class-1 SCUBA Galaxies [68,69]), perhaps similar to the well-studied galaxy HR10 at $z = 1.4$ [70].

The next generation of submillimetre cameras like SCUBA-2 and eventually ALMA will provide information,

in particular positions, at a far greater level of detail than the results presented here. The redshift distribution of submillimetre sources may well turn out to be the most direct measure of the infrared Madau Plot.

2.4.1.1 Constraints from Radio Followup of Submillimetre Sources

Infrared galaxies that are luminous at submillimetre wavelengths have radio fluxes that are faint but detectable [71,72]. This means that accurate positions can be obtained which in turn means redshifts can be obtained. If this can be done for a complete sample of submillimetre sources down to very faint flux levels, we can then construct the infrared Madau Plot. To date this has been done for a sample of 8 mJy SCUBA sources [73], but these do not contribute significantly to the infrared background. A sample of more typical 1 mJy sources would be required; with SCUBA this can only be achieved with the aid of gravitational lensing by imaging sources behind massive clusters.

2.4.2 Constraints from infrared background and source counts

Far-infrared surveys (which need to be undertaken from space, since the earth's atmosphere is opaque for most of $40 - 1000$ μm) offer another direct method of finding infrared galaxies. To date, sensitivity considerations (see the *ISO* points on Figure 3) have resulted in these surveys finding only the most luminous sources.

The next generation of instruments on infrared satellites should be at least an order of magnitude more sensitive. Consider, for example, a "typical" infrared galaxy with an 850-μm flux of 1 mJy (see section 2.4.1). The flux density $S_\nu \sim L_\nu \sim \nu^{3.5}$ a modified Rayleigh-Jeans spectrum for typical dust [31]. Therefore the 160-μm flux is 350 mJy (independent of redshift). These sources should be easily detectable with $SIRTF$/MIPS, which has a 5σ sensitivity at 160 μm of 50 mJy for a 500 second exposure (this is confusion-limited [74]). The poor resolution ($\lambda/2D = 19''$ at 160 μm for the 85 cm telescope) and large pixel size ($16''$) may, however, prevent straightforward identifications of the infrared sources. Redshift determinations will then be difficult and it will not be possible to construct the infrared Madau Plot from these observations alone. Observations with $SIRTF$/MIPS at 24 μm and 70 μm could help in this regard (the pixel size at these wavelengths is smaller and the resolution is better) but sources at high redshift and/or with only very cold dust may well go undetected at these shorter wavelengths.

2.4.3 GRB host galaxies

Gamma-ray bursts (at least the long-duration ones which last longer than 2 seconds) seem to come from massive collapsing stars. If the proportion of collapsing stars that become GRBs is roughly constant from one star-forming region to another (a major assumption), then the redshift distribution of GRBs tells us the star formation history of the Universe.

This assertion is based on various pieces of circumstantial evidence which when combinrd seem to be reasonably compelling:

1) GRBs tend to happen in galaxies with high star formation rates. Often these have been identified as blue star-forming galaxies at high-redshift, perhaps similar to local HII galaxies [75]. Most compelling, however, is that GRBs have now been seen in four infrared galaxies with huge star formation rates: GRB 980703, GRB 010222, GRB 000418, and GRB 000210 [10].

2) On theoretical grounds, a natural mechanism for producing a long-duration burst is the cataclysmic collapse of a massive star leading to a hypernova-type explosion [76].

3) On two occasions iron-line and edge features have been identified which are associated with GRBs [77,78] suggesting a link with supernovae and therefore with collapsing massive stars.

4) On four occasions, a red component with an optical flux consistent with that of a supernova was discovered several weeks after the burst (e.g. ref. 79).

One additional result that is extremely important is:

To date, three out of the four GRBs – 980703, 010222 and 000418 – that have happened in infrared-luminous galaxies have had bright optical afterglows

This means that these GRBs and their host galaxies can have their redshifts measured – for example, by the presence of absorption lines from the host galaxy in the afterglow spectrum. In turn, this means that we can measure the redshift distribution of *all* gamma ray bursts with optical afterglows, including the ones in infrared as opposed to optical galaxies.

We can directly compare the redshift distribution of GRBs to the predictions from models of the cosmic star formation history. All the bursts with redshift measurements to date are listed in Table 2 [80]. A comparison with current data is shown in Figure 4.

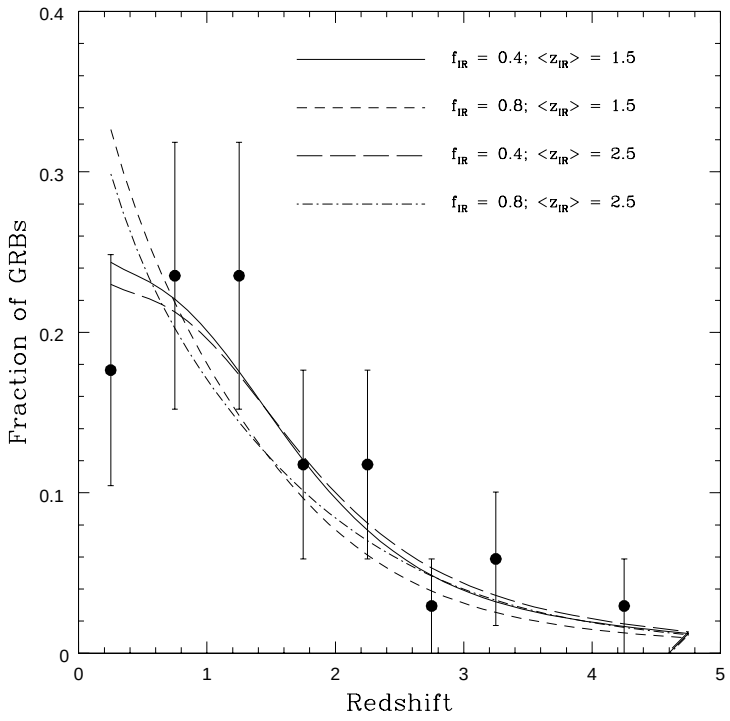

Figure 4: The redshift distribution of GRBs compared with predictions from different models of the cosmic star formation history. The data points represent the 34 bursts to date with redshifts known to better than 0.25. The lines represent different models of the cosmic star-formation history, consisting of a contribution from ultraviolet-bright galaxies (the optical Madau plot, from ref. 23) and a contribution from infrared-bright galaxies. The infrared bright galaxies are assumed to have a gaussian redshift distribution with mean $< z_{\rm IR} >$, variance $\sigma_z = 0.5$, and to contribute a fraction $f_{\rm IR}$ to the total star formation. The calculation of the lines further assumes that the number of GRBs per unit mass converted into stars is not a strong function of redshift and that GRBs have a luminosity function $\phi(L)$ where $\int_{4\pi d(z)^2 f_{\rm lim,det}}^{\infty} \phi(L) {\rm d}L$ does not vary strongly with redshift – all the relevant GRBs were Beppo Sax or HETE-2 detections.

Table 2

Gamma Ray Bursts with Redshift Measurements

Burst	Redshift
GRB 970228	0.695
GRB 970508	0.835
GRB 970828	0.96
GRB 971214	3.42
GRB 980326	~ 1
GRB 980329	< 3.9
GRB 980425	0.0085
GRB 980703	0.97
GRB 990123	1.60
GRB 990506	1.30
GRB 990510	1.62
GRB 990705	0.86
GRB 990712	0.43
GRB 991208	0.71
GRB 991216	1.02
GRB 000131	4.5
GRB 000210	0.85
GRB 000214	$0.37 < z < 0.47$
GRB 000301C	2.03
GRB 000418	1.12
GRB 000911	1.06
GRB 000926	2.07
GRB 010222	1.48
GRB 010921	0.45
GRB 011121	0.36
GRB 011211	2.14
GRB 020405	0.69
GRB 020813	1.25
GRB 021004	2.3
GRB 021211	1.01
GRB 030226	1.98
GRB 030323	3.37
GRB 030328	1.52
GRB 030329	0.168
GRB 030429	2.65

For such a comparison to be meaningful we need to make some assumptions:

1) we must assume some redshift-dependance on the fraction of massive stars which eventually generate GRBs. One extreme situation is that this fraction is independent of redshift – this may happen if the stellar IMF is universal and if mass is the main stellar parameter in determining whether or not a star becomes a GRB. The other extreme would be a situation where some redshift-dependant parameter (possibly metallicity) is the most important issue in determining whether or not a star becomes a GRB.

2) a GRB luminosity function must be assumed. One extreme situation might be to assume a δ-function at high luminosities – then we observe all GRBs, whatever their redshift. The other extreme would be a luminosity function

that is steeply rising at low luminosities. Then, any flux-limited sample of GRBs would be dominated by nearby GRBs of low intrinsic luminosity.

It is clear from Figure 4 that the current data do not provide any meaningful constraints on the models because the Poisson errors are far too large. Nevertheless, the fact that this method is sensitive to star formation in both ultraviolet and infrared galaxies makes it very attractive.

The areas of study required to turn this into a profitable method are:

• Very many more GRBs with redshifts need to be observed. Several hundred are required if we are to distinguish between the models in Figure 4. The $SWIFT$ satellite should provide this.

• The requirements for generating a GRB need to be understood so that assumption 1) can be tested. This will probably come from both theoretical modeling and observations of the environments in which GRBs occur.

• The gamma-ray luminosity function of GRBs needs to be measured, since in order to place specific models on Figure 4 we need to know this. Estimates of the luminosity function can be made from the flux statistics of bursts with measured afterglow redshifts [81].

• Many GRB host galaxies should be seen at infrared wavelengths by $SIRTF$. This is be a useful test of the whole pictures.

In summary, this seems to be a useful method although much additional data is needed before it can provide an accurate measurement of the cosmic star formation history. The optical part of the cosmic star formation history is already reasonably well established. The infrared part will come from ALMA. In the meantime, the GRB redshift distribution should provide interesting insights. In the long term (post-ALMA) it should provide a useful consistency check and will probably tell us something about the physics of GRBs.

2.5 Obscuration Extent

Given that most of the star formation in the Universe seems to be taking place in infrared galaxies, it is worth addressing the issue of how obscured this star formation is. Figure 5 shows a rough analysis.

The symbol "UV" represents the location of star-forming galaxies that are bright at rest-frame ultraviolet wavelengths; these are what generate the optical Madau Plot. At low redshift, the most luminous examples of these are late-type spiral e.g. Sc galaxies. At high redshift, these are Lyman-break galaxies. These objects have moderate or little obscuration ($A_V \leq 1$ mag typically), moderate or low star-formation rates (< 10 $M_\odot$ yr^{-1} normally, although a few have star-formation rates greater than this), and consequently low submillimetre fluxes (typically below 0.1 mJy). Consequently they occupy the bottom left corner of Figure 5.

The symbol "C2" represents the location of Class-2 SCUBA galaxies. These are luminous submillimetre source with high star formation rates that are also luminous at optical wavelengths. The fact that the star formation rate derived from optical measurements is comparable to the star formation rate derived from submillimetre measurements means that the star formation in these galaxies is only lightly obscured and hence they occupy the top left corner of Figure 5.

Most of the star formation probably happened in infrared galaxies, the ones that dominate the infrared background ("IRB"). Suspected examples are the three GRB host galaxies ("GRBh") described in the previous section. That the afterglows were able to emerge from the dusty host galaxies follows from the high specific intensity of the radiation source. It also tells us that the obscuration in the host galaxies, while wiping out most of the ultraviolet light, cannot be *too* severe. For example, were the hosts to be like local ultraluminous galaxies such as Arp 220 ("ULIG") the afterglows would not have emerged – there are tens of magnitudes of visual extinction to the cores of these galaxies, which is where all the energy is being generated.

The line-of-sight extinction to a GRB is, however, complicated by local physical processes. High-energy radiation from the GRB may heat and sublime nearby dust [82,83,84,85], but since the X-ray/UV flux $\sim d^{-2}$, dust grains at $>>$ 10 pc from the GRB are unaffected [82], and it is unlikely that the GRB can affect the absorption properties of dust on the scale of an entire galaxy.

So it appears that the infrared GRB hosts are quite unlike local ultraluminous galaxies. They are also different from Class 2-SCUBA galaxies since their optical fluxes are low. They are presumably some intermediate type of galaxy.

This is also what is suggested from evolutionary arguments [60]: only about 1% of the stars in local galaxies

are found at densities above 100 $M_\odot$ Mpc^{-3}. This is gas density in the cores of local ultraluminous galaxies like Arp 220 [86], which is where most of the energy is generated.

There are, however, three bursts which could have host galaxies similar to local ULIGs. These are the dark bursts GRB 000210, GRB 970828 and GRB 990506, which all had radio but not optical afterglows. In these cases the optical afterglow could have been extinguished by a dense interstellar medium. This possibility is further suggested for GRB 970828 by the observation is a merging/interacting system [87], like local ULIGs. Additionally GRB 000210 is in an infrared-luminous galaxy that is not very luminous at rest-frame optical wavelengths [88], again like local ULIGs.

The bursts GRB 990308, GRB 980329 and GRB 980326 all had extremely faint host galaxies but had optical afterglows [80] so these could perhaps be some intermediate kind of galaxy between those described in the previous paragraph and infrared galaxies like the host galaxy of GRB 980703.

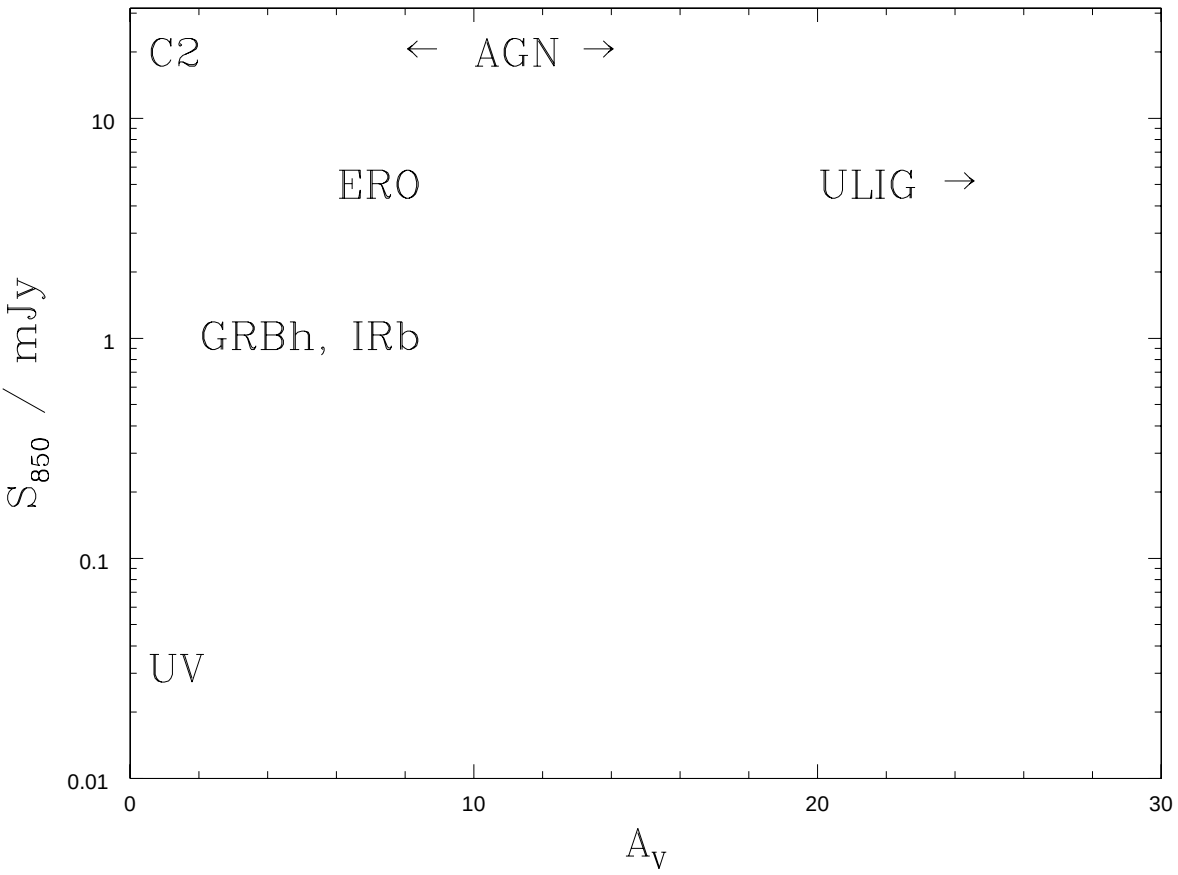

Figure 5: Cartoon showing the total obscuration, parameterized by the V-band extinction A_V and the submillimetre flux S_{850} for various extragalactic objects. See the text for details.

One more, independent, piece of evidence that suggests GRB host galaxies exhibit only modest obscuration is the analysis of Galama & Wijers [83]. They show that the column densities of gas in GRB host galaxies are typically $10^{22} - 10^{23}$ cm^{-2}, higher than in spiral galaxies like the Milky Way, but lower than in the dense molecular cores of local ULIGs like Arp 220.

In summary, there is considerable evidence that the star formation in the infrared galaxies which dominate the infrared background and are likely to produce most of the stars we see locally is only lightly obscured. There must be some obscuration so as to (i) generate the high infrared luminosities, (ii) extinguish sufficient rest-frame ultraviolet light to prevent the galaxies from being luminous in optical samples, and (iii) be consistent with column densities of $10^{22} - 10^{23}$ cm^{-2}. There cannot be too much or (i) the optical afterglows would not emerge and (ii) too many stars in local galaxies would reside at densities well in excess of 100 $M_\odot$ pc^{-3}.

EROs are somewhat more obscured than these infrared galaxies since the optical radiation (but not the near-infrared radiation) is completely extinguished – the GRB host galaxies described in the previous section all had optical detections, although they were faint. They also have slightly higher submillimetre fluxes: the three EROs discovered by Smail et al. [68] and Gear et al. [69] have (unlensed) 850-μm fluxes of 8.6, 1.6, and 8.8 mJy, whereas the infrared background is dominated by sources with fluxes closer to 1 mJy. The EROs therefore lie slightly upwards and to the right of the GRBh/IRB point on Figure 5; presumably they are a somewhat more obscured version of the more common type of infrared galaxy indicated by the "GRBh" symbol.

Active galactic nuclei (AGNs) represent some of the most luminous objects at optical [89], infrared [90], and submillimetre wavelengths. Ultimately this is because accretion onto a black hole is about 100 times more efficient at generating photons per unit mass than star formation. AGNs occupy the upper region of Figure 5 whether they are discovered by optical [91] or submillimetre [92] measurements. It is possible that the horizontal position of a particular object is determined by its evolutionary state. In the scheme of Sanders et al. [37,38] quasars form by the evolutionary sequence: cold ULIG (e. g. Arp 220) → warm ULIG (e. g. Mrk 231) → infrared quasar (e. g. I Zw I) → optical quasar (e. g. 3C 273; the most massive examples of these may be radio-loud, particularly in the late phases of evolution). On moving along this sequence, increasing amounts of dust are blown away from the central regions as the central black hole grows in size and the temperature increases. A given AGN therefore moves to the left on Figure 5 as it evolves. When the objects are very cold, note that a starburst, not an AGN, is likely to be the instantaneous power source (see ref. 93) and the models of Rowan-Robinson & Efstathiou [94].

2.6 Star Formation Rate Distribution Function

A useful quantity to consider is the star formation rate distribution function (SFRDF) in galaxies, defined where SFR dSFR is the number of galaxies with star formation rates between SFR and SFR+dSFR. The SFRDF tells us the sizes of the galaxies in which stars form. This is proportional to the ultraviolet luminosity function for optical galaxies at low [14,15] and high [49] redshift. For infrared galaxies, the SFRDF can be determined at low redshift from the infrared luminosity function (e. g. ref. 95), once the contribution for infrared emission from optical galaxies ($R > 0$) is subtracted.

The high infrared background means that the importance of the infrared SFRDF relative to the optical SFRDF must evolve strongly with redshift [32], but it is difficult to quantify at redshifts $z > 0.5$, which is where most cosmic star formation is happening. It is very probably top-heavy compared with the optical SFRDF, since (i) most of the high infrared background is generated by sources with $S_{850} = 1$ mJy which have star formation rates (~ 100 $M_\odot$ yr^{-1}) in excess of the most luminous optical galaxies, and (ii) the four infrared galaxies discovered as GRB host galaxies [10] all had star formation rates this high.

At the highest luminosities, many infrared sources may well be AGNs so that establishing the SFRDF at the extremely-high SFR end may be difficult.

This means that most of the stars that we see in local galaxies formed within big galaxies. The SFRDF is related to the local luminosity function, but not directly, since mergers between stellar systems produce final galaxies (which is what the local luminosity function measures) bigger than the progenitors (which is what the SFRDF measures). The top-heaviness of the local luminosity function compared to the SFRDF is therefore an indication of the role of stellar-kinematic mergers of existing systems in producing local galaxies.

2.6.1 Absorption line systems

Star-forming galaxies presumably form from HI galaxies, so one might expect the mass function of HI clouds (seen in absorption in quasar spectrum) to be similar to the SFRDF. Lanzetta et al. [58] demonstrates that for the two to be consistent, more star formation is required than is seen in optical surveys. They suggest that much of the star formation is missing from these surveys at high redshift due to $(1 + z)^4$ cosmological surface-brightness dimming. Another possibility is that much of the star formation that we might expect to occur from the HI column density function is happening in infrared galaxies that are missing from the optical surveys altogether.

In any case, the concordance between the cosmological density Ω_* of stars at $z = 0$ and the integrated cosmological density $\Omega_{\rm HI}$ in HI systems at all redshifts ($\int_0^4 \Omega_{\rm HI}(z)\,{\rm d}z / \int_0^4 {\rm d}z \approx \Omega_*$; ref. 96) means that all stars that we see locally are made of hydrogen that was part of an HI cloud at some redshift, assuming that the atomic hydrogen got converted to stars on short timescales. The clouds at high redshift are simply acting as reservoirs.

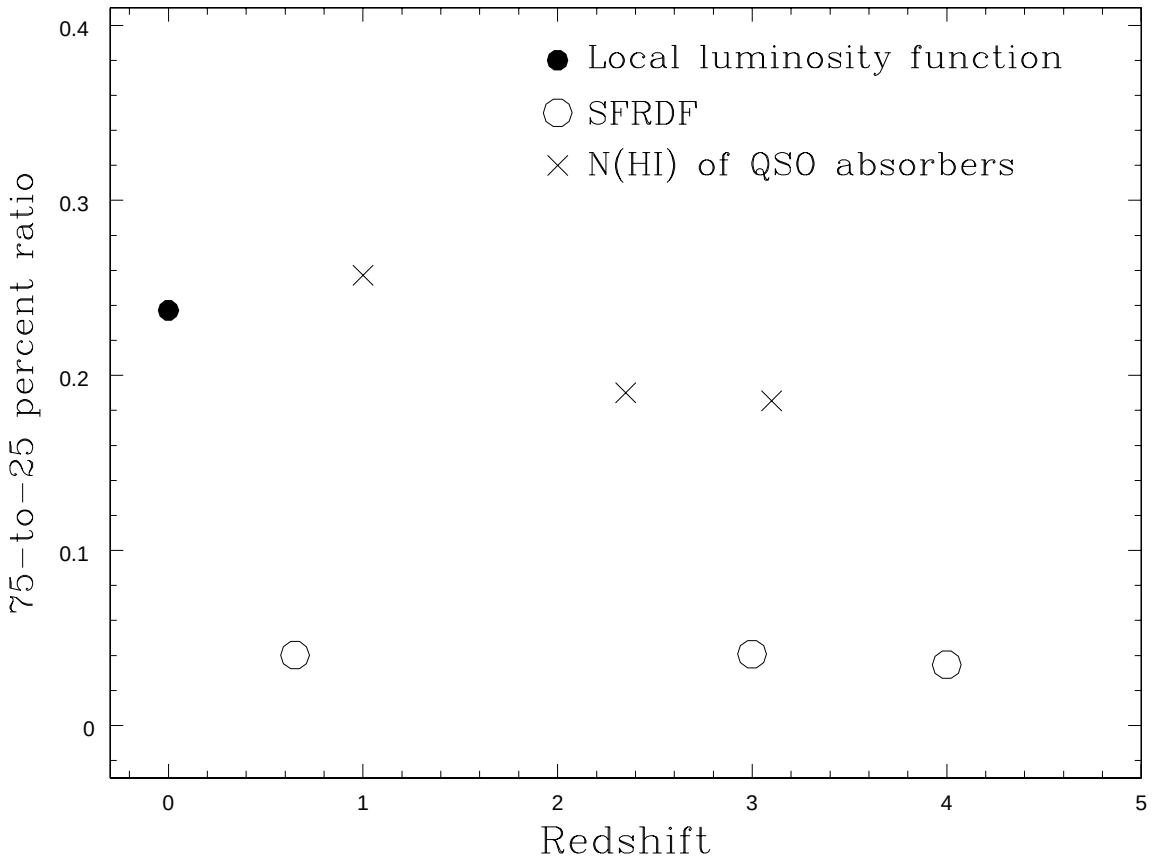

Figure 6: The 75-to-25-percent ratio for the quantities described in Section 2.6. The $z = 0$ galaxy luminosity function is from the SDSS collaboration [14]. The SFRDF and the redshift evolution of the infrared galaxy luminosity functin is from ref. 30. The $z = 3$ and $z = 4$ optical galaxy luminosity functions are those of Steidel et al. [49] and at $z = 0.65$ it is the 280-nm luminosity function of Cohen [47]. We assumed further that the stellar IMF is that of Kroupa et al. [34], that the infrared galaxies have dust temperatures of 37 K [32], that the infrared luminosity-to-star-formation-rate conversion factor for our IMF is 1.2×10^9 $L_\odot$ ${M_\odot}^{-1}$ yr [98], and that for optical galaxies, ultraviolet luminosities can be converted to star-formation rates using Kennicutt's relation [99]: SFR ($M_\odot$ yr^{-1}) $= 1.4 \times 10^{-28} L_\nu$ (erg s^{-1} Hz^{-1}) between 150 nm and 280 nm. The SFRDF is then $\mathrm{SFRDF_{opt}} + \mathrm{SFRDF_{IR}} = 0.00475\,(\mathrm{SFR}/2.8)^{-1.0}\,\exp(-\mathrm{SFR}/2.8)\,1/2.8 + 0.000865\,(\mathrm{SFR}/5.3)^{-0.1}\,\exp(-0.95\log_{10}(1+\mathrm{SFR}/5.3)^2)\,1/\mathrm{SFR}$ ($z = 0.65$); $0.0016\,(\mathrm{SFR}/6.1)^{-1.6}\,\exp(-\mathrm{SFR}/6.1)\,1/6.1 + 0.00088\,(\mathrm{SFR}/9.9)^{-0.1}\,\exp(-0.95\log_{10}(1+\mathrm{SFR}/9.9)^2)\,1/\mathrm{SFR}$ ($z = 3$); $0.0010\,(\mathrm{SFR}/6.1)^{-1.6}\,\exp(-\mathrm{SFR}/6.1)\,1/6.1 + 0.00078\,(\mathrm{SFR}/5.8)^{-0.1}\,\exp(-0.95\log_{10}(1+\mathrm{SFR}/5.8)^2)\,1/\mathrm{SFR}$ ($z = 4$) $M_\odot$ yr^{-1} Mpc^{-3}, where SFR is in units of $M_\odot$ yr^{-1}. Note that in all these functions $\mathrm{SFRDF_{IR}}$ is dominated by higher-SFR galaxies than $\mathrm{SFRDF_{opt}}$. The absorption-line system HI column density N(HI) distribution function is taken from the measurements of Péroux et al. [96].

The alternative view is that clouds at $z = z_1$ simply evolve into clouds at $z = z_2 < z_1$ and the atomic hydrogen in the clouds was converted to stars on long timescales, if at all (most hydrogen seen in HI systems at high redshift might subsequently have been ionized and be part of the intergalactic medium today). If this alternative view is correct then it is plausible that most hydrogen that is in stars at $z = 0$ never resided in an HI system at any redshift for any appreciable time.

The catchment volumes of the clouds at high redshift could correspond to present-day galaxies. A quantitative analysis is suggested. A useful mathematical construction that describes the shape of a function $f(x)$ of a measurable

variable x that is most reliably measured at large x is the 75-to-25-percent ratio

$$r = \frac{x_{75}}{x_{25}}$$

where

$$\int_{x_{75}}^{\infty} x\, f(x)\, \mathrm{d}x \;/\; \int_{0}^{\infty} x\, f(x)\, \mathrm{d}x = 0.75$$

and

$$\int_{x_{25}}^{\infty} x\, f(x)\, \mathrm{d}x \;/\; \int_{0}^{\infty} x\, f(x)\, \mathrm{d}x = 0.25.$$

A value $r \sim 1$ suggests $f(x)$ is top-heavy and high-x biassed. A value $r << 1$ suggests $f(x)$ is low-x biassed. Figure 6 shows r for a number of related functions.

Figure 6 shows that many of the stars in local galaxies reside in large systems and that much of the gas in high-redshift absorption-line systems also exists in large systems. Yet much of the star-formation in the Universe is not happening in the galaxies with the highest individual star formation rates. There are many possible explanations for this interesting result. Possibly the high-redshift absorption-line systems represent the catchment areas of systems that later become gravitationally bound to form galaxies, yet the stars were formed in smaller systems that later merged to form the final galaxies that we see today. This could be tested by studying the evolution of the correlation function between infrared galaxies and evolved stellar systems (seen in near-infrared surveys), the evolved stellar systems being the end-products of infrared galaxies which have completed their star formation. The correlation function between infrared galaxies and other infrared galaxies may be useful too but on the other hand may be very small if infrared galaxies within a particular catchment volume burst at different times For example, the luminous galaxy SMM J14011+0252 [25] appears to be a many-component system at optical wavelengths, and it is possible that one component contains an obscured starburst whereas the others are evolved stellar systems.

The idea that the HI clouds are systems that have yet to collapse and form galaxies is also suggested by measurements of abundances in damped Lyα systems at high redshift [97]. The abundances in the clouds are lower than those of Milky Way stars with ages comparable to the cosmological ages of the clouds. This suggests that at the cosmological ages in question galaxies like the Milky Way, whose formation is traced by the SFRDF, have already formed (presumably in smaller units), but the gas in the HI systems has not yet been converted into stars in galaxies yet.

2.7 Summary of Section 2

The main result of this section is that most of the star formation in the Universe is happening in infrared rather optical galaxies with star formation rates of about 100 $\mathrm{M}_{\odot}$ yr^{-1}. Most of this star formation is unaccounted for in optical surveys because of internal extinction, but this internal extinction is not large; a number of independent arguments suggest that it is no more than a few magnitudes in A_V. The host galaxy of GRB 980703 appears to be a good prototype. The starbursts in these galaxies are likely to be short-lived [100].

The precise fraction of star formation f_{IR} that happened in infrared galaxies is uncertain but it is probably above 50 % [30].

One of the main constraints on f_{IR} come from the spectrum of the extragalactic background light. In particular, our estimate of f_{IR} will be too high if infrared part of the EBL spectrum is overestimated, perhaps due to contamination from a warm Galactic component [101].

It will also be too high if the optical part of the the EBL spectrum is underestimated, as would happen if there exists significant amounts of optical flux originating from the outer parts of galaxies. This would contribute to the EBL [102], but would not be accounted for in determinations of the EBL obtained by summing contributions from resolved sources. It would also be unaccounted for in determinations of the optical Madau Plot, particularly if the star formation is happening at high redshift where $(1+z)^{-4}$ surface-brightness dimming is important [58]. If this were the case, there would need to be very many stars or their remnants today in the outer parts of galaxies and their halos, like the cold white dwarfs observed by Oppenheimer et al. [18].

Yet another issue which could lead to an overestimate of f_{IR} is the temperature T of dust-enshrouded starbursts. If they are significantly lower than 40 K, then the star-formation rates implied by radio measurements

for galaxies like the host galaxy of GRB 980703 will be too high. The logic is as follows. The temperatures are determined by modelling, number counts, the EBL, and SEDs for a few luminous sources [32]. But if the bulk of the energy is produced by sources of moderate luminosity (like the SCUBA 1 mJy sources) that are colder than the more luminous sources that contribute to the bright end of the counts and have well-determined SEDs, then the bolometric luminosities of the moderate-luminosity starbursts ($L_{\rm bol} \sim S_{850}\, T^{4.5}$) and their star-formation rates (SFR $\sim L_{\rm bol}$) will be overestimated. When we then determine SFR from a radio flux for any galaxy based on the radio-submillimetre flux calibration [71,72], it will be too high. When summed over the entire infrared poplation based on flux and/or background measurements, the consequent value of $f_{\rm IR}$ will be an overestimate.

3 THE LOCAL GALAXY POPULATION

3.1 Galaxy types and stellar populations

3.1.1 Disks and Spheroids

Most familiar luminous galaxies are giant galaxies, either ellipticals or spirals.

Giant ellipticals have high brightnesses at their centres and absolute B magnitudes between about -25 and -15. Elliptical galaxies are featureless, with brightness profiles that are high in the center and lower far away from the center. They are red and metal-rich (typically 1 – 2 $Z_\odot$), consisting mainly of old stars.

Spiral galaxies have absolute B magnitudes between about -24 and -18. They often look smooth near their centres (where the brightnesses are highest) and have spiral arms at large radii from ther centres. The spiral arms are often irregular in form and one can see many condensations or knots, like HII regions which are making stars. Spiral galaxies can generally be separated into bulges and disks [103,104]. The bulges are predominantly composed of old, red Population II stars. The disks contain young, blue Population I stars, particularly in spiral arms where there is considerable ongoing star formation.

The familiar Hubble sequence Sa→Sab→Sb→Sbc→Sc→Scd→Sd is used for categorizing spiral galaxies. The main parameter which varies along the sequence is the relative luminosities of the bulge and disk [105,106]. Galaxies classed Sa have substantial bulges. Galaxies classed Sd have no bulges. Familiar examples are M81 (Sab), M31 (Sb), the Milky Way (Sbc), M51 (Sbc), M101 (a luminous Scd) and M33 (a low-luminosity Scd).

A less common type of giant galaxy is the peculiar galaxy. They are often systems of interacting galaxies (e.g. ref. 107) or galaxies that have undergone a recent interaction. These galaxies normally have SEDs which peak at infrared wavelengths. Familiar examples are the Antennae (NGC 4038/9), NGC 7252 and Arp 220.

Galaxies with absolute blue magnitudes fainter than -18 are mostly dwarf galaxies. There are two kinds: red dwarf elliptical (dE) galaxies with old stars, smooth morphologies and no detectable HI gas, and blue dwarf irregular (dIrr) galaxies which have younger stars, complex morphologies (often they are star-forming condensations embedded within a luminous matrix) and appreciable HI gas. The dwarf irregulars are generally metal-poor ($<$ 0.1 $Z_\odot$) whereas most dwarf ellipticals have higher metallicities (although still lower than those of giant elliptical galaxies). The dEs in the Local Group cover a large range in absolute magnitude, from NGC 205 ($M_V = -15$) to Draco ($M_V = -8.5$). There are also a number of dIrr galaxies in the Local Group, like the Large and Small Magellanic Clouds (LMC and SMC) and NGC 6822.

If a galaxy has a bright quasar at the center, the quasar is usually so bright that one cannot see the rest of the galaxy. Such objects therefore look pointlike.

Finally, there do exist other, rarer, less classifiable galaxies, like giant low-surface-brightness galaxies that can barely be seen above the sky. Malin 1 [108] is the prototype of this kind of galaxy.

3.1.2 Halo Stellar Populations and MACHOs

Galaxy halos mostly consist of dark matter, but there are small number of field halo stars. These are Population II stars, identified in the Milky Way by their halo kinematics. The fraction of the Galaxy's stellar mass that is in the halo is very small (a few percent or less), but the exact mass of the halo stellar component is known very imprecisely. Freeman & Bland-Hawthorn [109] suggest a total stellar halo mass of about 10^9 $M_\odot$, but Binney & Merrifield [110] point out that many of the blue horizontal-branch stars used to estimate the halo mass might in fact be thick disk members and that the field halo stellar mass may be only about 10^8 $M_\odot$.

Another stellar mass component of the Galactic Halo is the globular cluster (GC) population. These are about 150 dense, very old Population II systems of characteristic masses $10^5 - 10^6$ $M_\odot$. Individual globular clusters are susceptible to tidal disruption (e. g. Pal 5; ref. 111) and much of the field halo could have been generated in this way, although for most halo stars to have been part of a GC at some time in the past the GCs would have to have been very much more numerous then than now.

In an interesting recent development, Oppenheimer et al. [18] have discovered a number of cold (presumably old) white dwarfs in the Milky Way halo. They are almost dark: the prototype WD0346+246 has a mass of about half a solar mass but a V absolute magnitude of about 17 [112]. Oppenheimer et al. [18] suggest that about 2% of the halo dark matter could be in the form of these white dwarfs. If a contribution from helium white dwarfs (which are not detected by Oppenheimer and collaborators) is included, this fraction could be higher. The total mass of the progenitors of these stars, massive stars which would have completed their evolution and become white dwarfs long ago and since cooled, is then comparable to the mass of stars in the rest of the galaxy. The mass in these remnants is far greater than that predicted from the extrapolation of the normal field halo star mass function.

If the Milky Way is typical of other galaxies, then an appreciable fraction of the star formation in the Universe would then have produced stars which reside in galaxy *halos*. This would be quite remarkable in light of our other knowledge of the galaxy formation process so it is worth examining possible sources of systematic error in the derivation of the 2% fraction quoted above. Possible systematic errors could arise from:

(1) contamination from a thick disk [113];

(2) contamination from stellar remnants ejected from the Galactic disk by 3-body or multiple encounters [114], or the remnants of donor stars from disk Type Ia supernovae [115];

(3) the derivation of density in the V/V_{max} method used by Oppenheimer et al. [18] is sensitive to assumptions which are difficult to test about the joint proper-motion–luminosity distribution function of the subsample used to derive the density.

A second remarkable aspect of this result is that it would not be consistent with our picture of Galactic or cosmological chemical evolution [19]. The problem is that the white dwarf progenitors would eject a large mass of metal-rich gas. This gas is not present in the Milky Way, nor (should it have been ejected by a galactic wind) in Lyman-α forest clouds.

Additionally, the results from the MACHO microlensing collaboration are now available. The purpose of this project was to look of lensing events by dark objects in the outer Milky Way halo where the sources were LMC stars. The results are [116]: between 8 % and 50 % of the dark halo consists of objects with characteristic masses between 0.15 $M_\odot$ and 0.9 $M_\odot$. This mass may or may not be baryonic. If it is, many of the baryons in the Universe will be in the form of MACHOs. Because the mass range above corresponds to stellar masses, MACHO production, probably in galaxy halos, would then dominate the cosmic star formation history. This would again be a remarkable result, given what we know about star and galaxy formation.

The important issue then is to determine whether or not MACHO production is or is not represented in the Madau Plot, and this depends on the nature of individual MACHOs themselves. Possible candidates include:

(1) normal hydrogen-burning stars. This would appear to be ruled out as the MACHO results would overpredict the observed field halo star number density by at least an order of magnitude;

(2) non-hydrogen-burning stars. Brown dwarfs are stars too low in mass ($< 0.08\,M_\odot$) for hydrogen to ignite, but the MACHOs are more massive than this. If somehow stars with masses $\sim 0.5\,M_\odot$ can form but fail to ignite hydrogen, these could be MACHOs if they exist predominantly in galaxy halos. Possible mechanisms for forming such objects are described by Hansen [117] and Lynden-Bell & Tout [118], based on the collapse of thermal instabilities in primordial gas. In this instance the MACHOs would contribute significantly to the baryon mass density of the Universe, but not to the Madau Plot since they would never generate radiation at any wavelength;

(3) cold white dwarfs. Although they have the right masses, the mass density of cold white dwarfs measured by Oppenheimer et al. [18] appears too low for most MACHOs to be this kind of object. More generally, stellar remnants that form as the end stages of stellar evolution are unlikely to be MACHOs if they as numerous as implied by the microlensing results, because they would then produce more helium and heavy elements than is consistent with observation [19,119];

(4) cold dark matter condensations. Most of the halo appears to be made of dark matter that is probably cold. The behaviour of instabilities in a dark matter fluid in which is embedded large number of stars is complex, particularly if the stars have a different velocity structure to the dark matter. If the instabilities grow to masses comparable to those of the stars, they could be MACHOs. Because the dark matter in this case would not be baryonic, the

formation of these MACHOs would not be represented on the Madau Plot. Note the importance of a field halo star population in such a scenario. In this scenario, galaxies lacking a substantial field halo population (like Local Group dwarf ellipticals) would not contain many MACHOs;
(5) quark nuggets [120] or other exotic forms of dark matter. Again, if the dark matter is of this type its formation would not be included in the Madau Plot. But there would certainly be an element of coincidence at work here: it is not clear why the dark matter would clump on exactly the same mass scales as normal stars and their remnants.
Finally, it is worth remarking that the interpretation of the MACHO observations is subject to numerous potential systematic errors (e.g. anomalous LMC substructure, self-lensing); so the numbers given in the previous paragraph could in principle be too high. The EROS microlensing project [121] has found less candidate events than the MACHO project and as more data is taken and analysed, potential systematic errors associated with particular lines of sight will become better understood.

3.2 Luminosity Functions

The total luminosity function of galaxies is well described by a Schechter function (Equation (1). One of the results from the large redshift surveys that are currently in progress [14,15,47,122,123,124,125,126] is a precise measurement of the galaxy luminosity function of the local Universe.

3.2.1 Type-specific Luminosity Functions

If the luminosity function is broken down into the contributions from different types of galaxies, more complex patterns emerge [13,127]. The luminosity functions of E, S0, Sa, Sb, Sc, and Sd galaxies are described approximately by Gaussian functions, in order of decreasing mean luminosity. The luminosity functions of dIrr and dE galaxies are described by Schechter functions of comparable characteristic luminosity. It is further possible to perform bulge-disk decompositions and to obtain the luminosity functions of different stellar populations, most significantly for the bulges and disks in Sa and Sb galaxies (the star-forming disk component is negligible in earlier-type S0 and E galaxies, and the bulge is negligible in later-type Sc and Sd galaxies). The luminosity functions for each stellar population can be converted from optical to near-infrared K-band (2.2 μm) luminosity functions using optical–near-infrared colours (e. g. ref. 128). The K-band luminosity functions are particularly useful since the K-band luminosities are not strongly affected by internal obscuration from dust within the galaxies ($A_K = 0.1 A_V$).

3.2.2 The Stellar Initial Mass Function

The luminosities of stellar populations depend mainly on the contributions from high-mass stars. In young Populations I these are blue OB stars. In old Populations II these are red giants and supergiants. The masses of the populations, however, depend primarily on the contributions from low-mass stars, whose observational signatures are weak.

A stellar initial mass function (IMF) $\xi(m)$ therefore needs to be *assumed* when comparing observational quantities which depend on luminosities to theoretical quantities which depend on masses. Population masses, mass-to-light ratios, and star formation rates all depend on the mass integral $\Xi_M = \int_0^\infty m\,\xi(m)\,\mathrm{d}m$.

Luminosities, on the other hand, are closely related to the same integral performed above some threshold mass m_l: $\Xi_L = \int_{m_l}^\infty m\,\xi(m)\,\mathrm{d}m$.

The general form of the IMF is a steep power law at high masses which flattens at 0.5 – 1 $\mathrm{M}_\odot$. The IMF does not appear to vary significantly from place to place [129]. The most simple approximation to the IMF is a single power-law $\xi(m) \propto m^\alpha$ [130,131]. More complex functions that are derived from direct fits to data are the IMFs of Gould et al. [132] and Kroupa et al. [34]. The Kroupa et al. [34] IMF has the advantage of a simple analytic form:

$$\xi(m) = \begin{cases} 1.87\,\xi(1)\,m^{-1.3} & 0.08 \leq \mathrm{m} < 0.5, \\ \xi(1)\,m^{-2.2} & 0.5 \leq \mathrm{m} < 1.0, \\ \xi(1)\,m^{-2.7} & 1.0 \leq \mathrm{m}, \end{cases} \tag{3}$$

where m is the stellar mass in units of the solar mass.

A commonly used IMF is the Salpeter [130] IMF with $\alpha = -2.35$ and a lower-mass cutoff of $m_l = 0.1$ $\mathrm{M}_\odot$. Let us call the mass-integral of this IMF Ξ_0. If then lower-mass cutoff is raised to 0.15 $\mathrm{M}_\odot$, then $\Xi = 0.87\,\Xi_0$. For

a Gould, Bahcall & Flynn [132] IMF below 1 $M_\odot$ and a Salpeter one above it, $\Xi = 0.60\,\Xi_0$ (see ref. 106). For the Kroupa, Tout & Gilmore [34] IMF with a lower-mass cutoff of 0.1 $M_\odot$, $\Xi = 0.45\,\Xi_0$. This is the IMF we assume elsewhere in this review. The reason that the mass integral is so much (about a factor of two) lower than the Salpeter one is the flattening of the IMF at low masses and the consequent absence of low-mass stars, the ones that dominate the mass integral.

3.2.3 Type-specific Mass Functions

The mass function of entire stellar populations may be derived by combining galaxy luminosity functions, bulge-to-disk ratios and population mass-to-light ratios Γ. This is done in Figure 7. The quantity $\Gamma \propto \Xi$, so each of the curves in Figure 7 scales with the value of Ξ appropriate to that population. If the IMF is universal, all curves scale by the same amount.

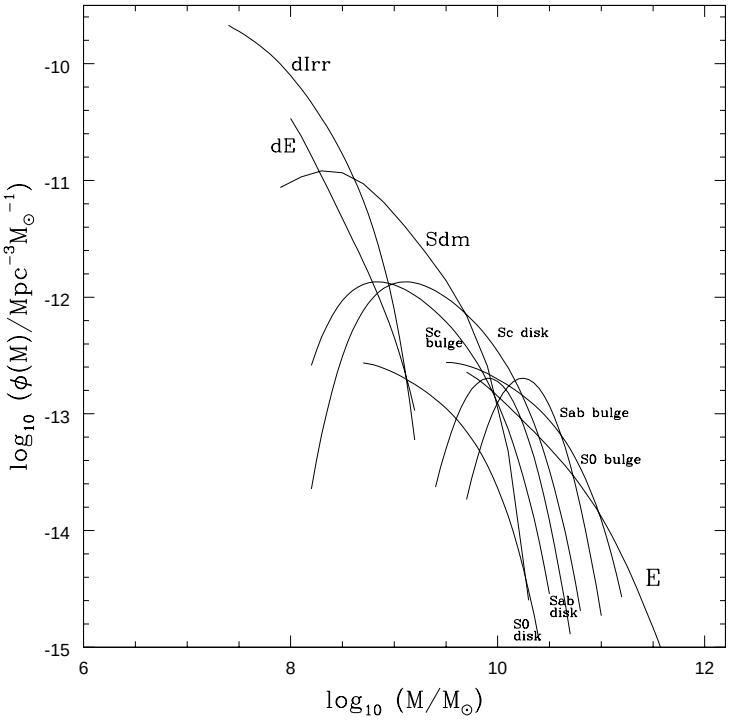

Figure 7: The galaxy mass functions $\phi(M)$ for elliptical (E), lenticular (S0), spiral (Sab, Sc, Sdm), dwarf irregular (dIrr) and dwarf elliptical (dE) galaxies. The bulge and disk component of the spiral and lenticular galaxies are considered separately. This figure is based on the luminosity functions of Binggeli et al. [13] and the mass-to-light ratios, bulge-to-disk ratios and cosmological luminosity density of Fukugita et al. [106]. The mass-to-light ratios used here are average values for classes of stellar populations (e.g. spheroids or disks). A more rigorous analysis would include the luminosity dependance of the stellar mass-to-light ratios ($M/L \propto L^{0.35}$; ref. 133, which follows from the fact that lower luminosity galaxies have lower metallicities [134].

Note that these mass functions apply to the stellar populations alone and are independent of the presence or absence of dark matter. Furthermore, for stellar populations the mass-to-light ratios are increasing functions of luminosity, but when the dark matter is included they become *decreasing* functions of luminosity [135] i. e. lower-luminosity galaxies are increasingly dark-matter dominated.

Figure 7 shows that the most massive systems are luminous elliptical galaxies. No spiral bulges or disks are as luminous as the most massive ellipticals. These massive systems probably turned their gas into stars very early in the history of the Universe. They have likely cleared out their catchment volume early on and have little or no gas left to form disks and/or turn into stars. This follows from the facts that (1) the earliest-forming systems have

had the most time to convert gas into stars, and (2) the most massive systems have large gravitational potential wells and so are particularly efficient at collecting gas, compressing it to high densities, and turning it into stars.

In clusters of galaxies (note that Figure 7 is appropriate for the field and is not relevant in this context), the supergiant cD galaxies are even more luminous than the most luminous field elliptical galaxies. These are probably formed by special cluster processes linked to the tidal disruption of individual cluster galaxies in the presence of the massive cluster dark-matter halo. This is inferred by:

1) the positions of cD galaxies in the precise centres of galaxy clusters;

2) the huge extended stellar halos around cD galaxies;

3) the high stellar velocity dispersions in the outer parts of cD galaxies [136], implying the presence of dark matter in amounts characteristic of galaxy clusters rather than individual galaxies.

Finally note that spheroid populations (ellipticals and bulges) have higher mass-to-light ratios than galaxy disks, by a factor of about 4. This is why there are comparable masses of bulge and disk in Sb and some Sc galaxies, even though the disks dominate the optical luminosities.

3.2.4 Low-luminosity and Low-surface-brightness Galaxies

One long-standing concern in extragalactic astronomy is that galaxies with extremely low surface brightnesses could dominate the luminosity density of the Universe [137]. These would missing from optical surveys because they are never visible above the night sky. Recent measurements have shown, however, that the contribution from galaxies with extremely low surface brightnesses has been shown to be small. These conclusions follow from deep optical surveys (the survey of Trentham & Tully [16] reaches nearly 29 R mag arcsec^{-2}). The results are particularly important at low luminosities, where most galaxies, like the Local Group dwarf spheroidals, are known to have low surface brightnesses [138]. These low-luminosity, low-surface-brightness dwarfs, like Draco [139], have high dark-matter fractions but their number densities are not high enough that their dark matter dominates the total mass density.

In the Local Group, incompleteness in the luminosity function due to our missing very low surface brightness objects is perhaps more of a concern since they cover such large areas of sky. Around M31 the census [140] appears to almost complete. Around Milky Way, new dwarfs like Cetus [141] are still being discovered, but these have absolute magnitudes fainter than $M_B = -11$, the magnitude limit of the luminosity function discussed in this section).

3.2.5 Environmental Effects

There is increasing evidence that the galaxy luminosity function is somewhat different in high density environments like galaxy clusters than in low density environments ("the field"). There appear to be two types of galaxy luminosity function – one for evolved regions (where the elliptical galaxy fraction is high, the galaxy density is high and the crossing time is short) like the Virgo Cluster and one for unevolved regions like the Ursa Major Cluster (an accumulation of about 80 spiral and lenticular galaxies; ref. 142) and the Local Group. The Virgo and Ursa Major LFs represent natural prototypes for the two kinds of luminosity function (see Figure 8) due to the small Poisson counting errors in the functions (ref. 143 for Ursa Major, ref. 144 for Virgo).

The main differences between the two are that (1) amongst the more luminous galaxies, the elliptical galaxy fraction is higher in clusters than in the field and (2) in clusters there are more low-luminosity dwarf galaxies per giant galaxy, although *all* environments are deficient in dwarf galaxies compared to the predictions from cold dark matter theory, which is otherwise very successful at explaining the properties of galaxies and their large scale distribution.

The preponderance of giant elliptical galaxies in clusters is probably due to ram-pressure stripping of gas in cluster galaxies by the hot intracluster medium and by the numerous galaxy-galaxy interactions in the history of cluster galaxies, particularly in the early stages of cluster assembly, before the galaxies acquired high velocities (due to the high cluster velocity dispersion).

The preponderance of dwarf elliptical galaxies in clusters is probably due to the fact that the stars in the dark halos surrounding dwarf galaxies formed at an earlier time than the stars in field galaxies. This is borne out by the red colours of cluster dwarfs compared to field dwarfs. The higher dwarf-to-giant ratios in clusters may be due in part to the fact that cluster dwarfs, unlike field dwarfs, formed prior to reionization [145], although it seems

likely that this is not the only important physical effect [146]. More generally, the conditions under which stars formed in galaxies in dense environments (that would later become galaxy clusters) in the early Universe is very likely different from the way stars formed in galaxies in normal, diffuse environments at late times.

In the context of the current discussion we are interested in the *field* luminosity function, not the cluster one. The fraction of the mass in the Universe in dense elliptical-rich clusters is small, perhaps not more than a few percent. But the first galaxies in the Universe to form probably exist in such environments today. These tend to be the easiest galaxies to study, particularly at high redshift, so care must be taken not to draw conclusions about cosmology from the properties of small numbers of extreme objects.

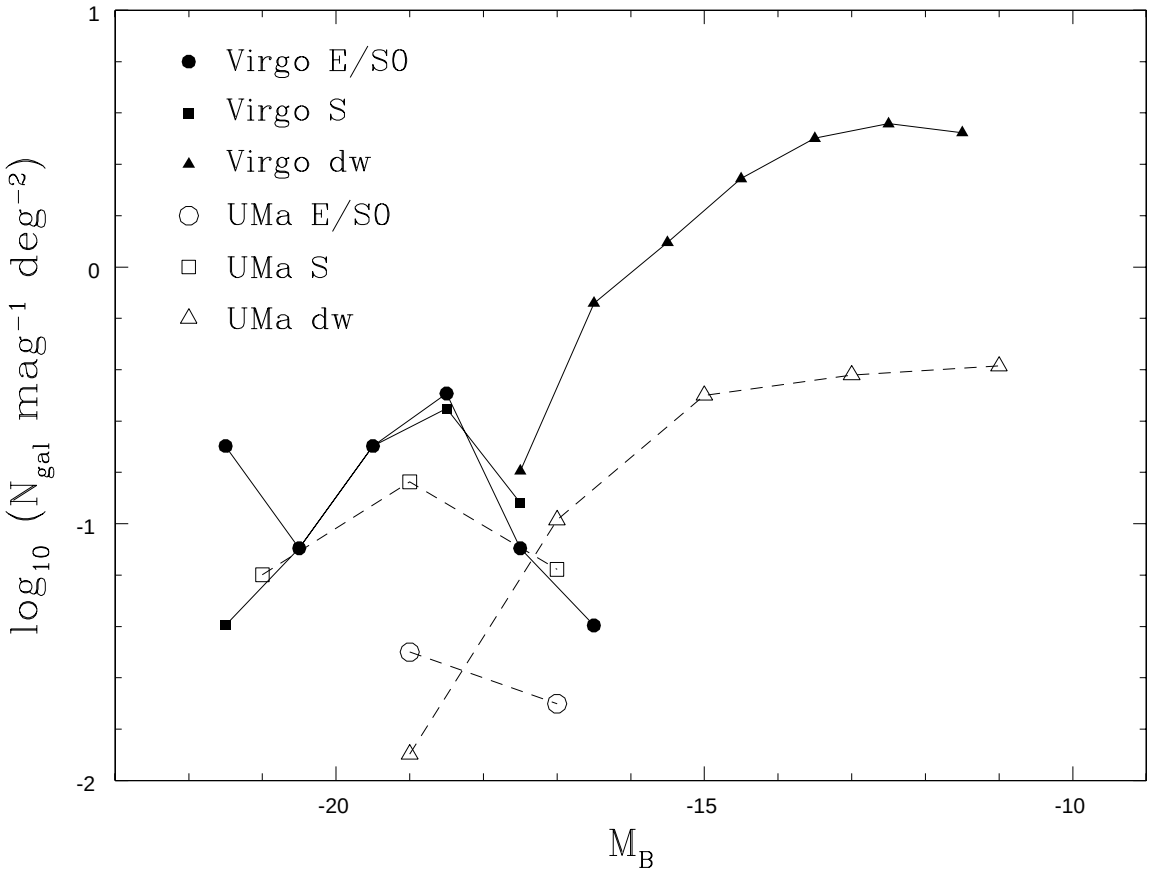

Figure 8: The galaxy luminosity function for the Virgo (filled symbols; ref. 144) and Ursa Major (open symbols; ref. 143) Clusters for elliptical/lenticular (E/S0), spiral (S), and dwarf (dw) galaxies.

3.3 Structural and Kinematic Parameters

Giant elliptical galaxies have brightness profiles well fit by a de Vaucouleurs $r^{\frac{1}{4}}$ law;

$$I(r) = I_e \, e^{-7.67\left(\left(\frac{r}{r_e}\right)^{\frac{1}{4}}-1\right)}, \tag{4}$$

where I_e and r_e are the effective brightness and radius. The structural parameters – the absolute magnitude, effective surface brightness, central velocity distribution, effective radius radius – of elliptical galaxies are described by the fundamental plane [147]. Importantly, as the luminosity of elliptical galaxies increases, their central surface brightness *decreases* (see Figure 9). Luminous elliptical galaxies like M87 are diffuse in their centre and are extremely large. Small elliptical galaxies like M32 are dense and bright in their centres and are extremely compact. The most luminous ellipticals also tend to have dense stellar cores. These are rarely isothermal [148] and have light profiles

that are flatter than an extrapolation of an $r^{\frac{1}{4}}$ law to small radii. Lower luminosity ellpticals tend not to have these cores; rather they have power-law brightness profiles that extend all the way to their centres [149]. More luminous ellipticals also tend to have isophotes that are boxy, lower-luminosity ellipticals that are disky [150].

The most luminous ellipticals are flattened by velocity dispersion anisotropy, lower luminosity ellipticals by rotation [151]. The cores in the luminous ellipticals are often kinematically decoupled from the rest of the galaxy (e. g. ref. 152) and can even be counter-rotating. Kinematic measurements [39,153] also infer the presence of supermassive black holes in the centres of elliptical galaxies, probably the remnants of dead quasars and AGNs. The black holes have masses roughly in proportion with the stellar masses of the *entire* galaxy: $M_{\rm bh} \approx 0.005 - 0.010\, M_*$ for our adopted (low-Ξ) IMF and cosmology.

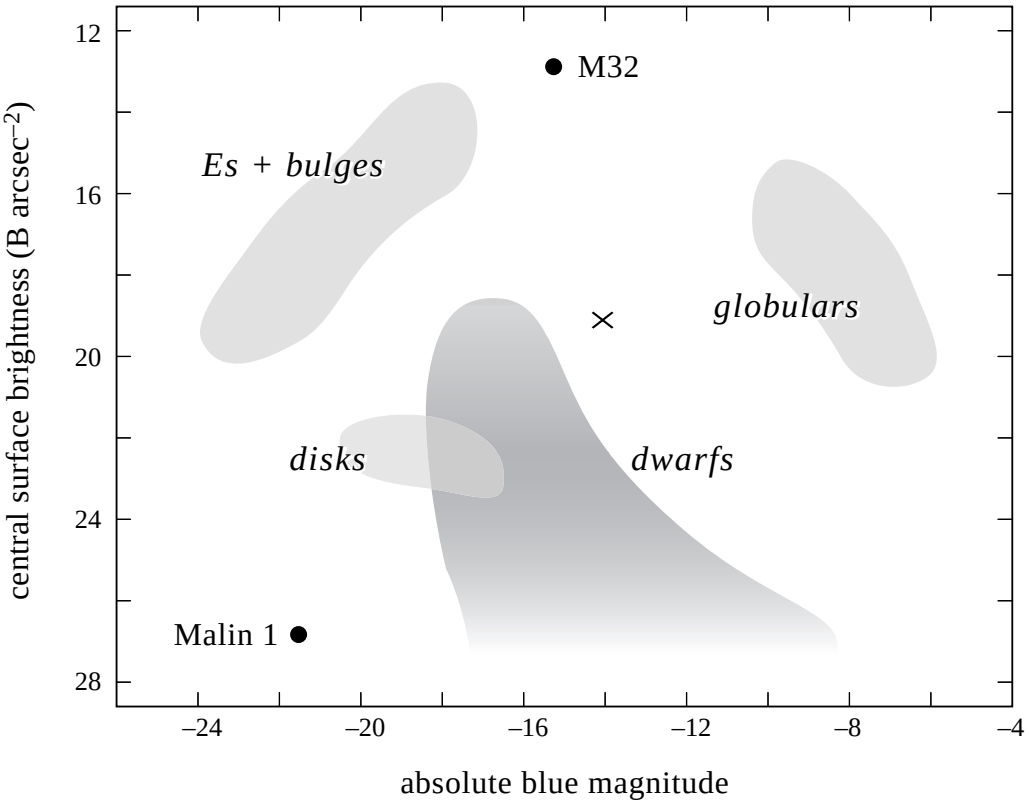

Figure 9: The absolute magnitude vs. central surface brightness relationship for various stellar systems, adapted from Binggeli [138]. Stellar systems do not normally occupy the regions between the shaded areas, notable exceptions being Malin 1 and M32. Another possible group of exceptions are star-forming compact galaxies, like Markarian 1460 [154]. For other examples, see the samples studied by Doublier [155] and Drinkwater [156,157].

Bulges of spiral galaxies are similar in many ways to low-luminosity elliptical galaxies. They have brightness profiles that follow a $r^{\frac{1}{4}}$ law, lie on the same fundamental plane as elliptical galaxies, are flattened by rotation as opposed to velocity dispersion anisotropy, and have black holes whose masses follow the same black-hole-mass vs. stellar mass correlation as elliptical galaxies.

The disks of spiral galaxies have lower surface brightnesses than elliptical galaxies and have brightness profiles which follow an exponential law:

$$I(r) = I_0\, e^{-\frac{r}{h}}, \tag{5}$$

where I_0 and h are the central surface brightness and scale length. Many disks have central surface brightnesses close to precisely 21.6 B mag arcsec^{-2} [158].

Dwarf galaxies also have exponential light profiles. They have decreasing surface brightness as they get lower in luminosity, a correlation in the opposite sense to that for elliptical galaxies. The faintest dwarf galaxies, Draco and Ursa Minor ($M_V = -9$), have very faint surface brightnesses indeed and are barely visible above the sky. Both types of dwarf galaxy have similar correlations of magnitude with surface brightness [159] and appreciable dark matter halos (e. g. ref. 139).

Globular clusters have light profiles that are well-fit by King models [160]. Like dwarf galaxies, they have decreasing surface brightness as they decrease in luminosity, but they do not have substantial dark matter halos and have much higher surface brightnesses than dwarf galaxies. Consequently they are easy to distinguish from dwarf galaxies although they have comparable optical luminosity. Globular clusters are spherical in shape and normally found in the halos of giant galaxies, sometimes far out in the outer halo e.g. the Pal Clusters and NGC 2419 [161] around the Milky Way. The formation mechanism for globular clusters is poorly understood [162] but there is evidence of a supermassive black hole in the centre of the Milky Way globular cluster M15 [163,164] and this may provide some important clues. Globular clusters that are unambiguously intergalactic have yet to be found, even in galaxy clusters [165].

3.4 Colour-magnitude Diagrams and Star Formation Histories of Local Group Galaxies

Detailed star formation histories are available for Local Group galaxies because individual stars can be resolved, even at the low-mass end of the main sequence. Some general results are summarized by Hodge [166]. Of particular note are

1) M31 and the Milky Way have quite different star formation histories. In M31 almost all the stars were made at early times. In the Milky Way many stars were made early on, but the star formation has continued to the present day, the current rate being about 1 $M_\odot$ yr^{-1};

2) the star formation in the Magellanic Clouds is extremely sporadic, with bursts happening on scales of 1 kpc separated by times of about 10^8 yr. When we look at most dIrr galaxies (like the Magellanic Clouds), we typically see a small number of extremely blue regions of enhanced star formation embedded in a blue luminous matrix of typical dimension 1 kpc. In order to generate this instantaneous view, the bursts must have lifetimes comparable to 10^8 yr and the young stars responsible for the blue light must form with such a high velocity that many are able to leave their birthsites before they die. There must also be a plentiful gas supply all over the galaxy to fuel this star formation. Note that dIrr galaxies are observed to be HI-rich;

3) Local Group dwarf elliptical galaxies have a wide variety of star formation histories. For example, in Ursa Minor all the stars are very old and metal-poor – indeed the colour-magnitude of this galaxy [167,168] looks similar to that of a Milky Way globular cluster. On the other hand, in Carina (e. g. ref. 169) most of the stars formed several Gyr after star formation began.

In the Local Group, M31 and the Milky Way are the only two luminous giant galaxies of type that dominate the local cosmic star formation rate. So we need to look beyond the Local Group if we wish to get colour-magnitude diagrams of typical luminous star-forming galaxies. The problem is that, for such galaxies, we can only resolve the most luminous stars (this is increasingly true with increasing distance and consequently with increasing sample size). In general, we must model star formation histories based on stellar evolutionary theory (that is well-tested in the Milky Way and Local Group), colour-magnitude diagrams of the most luminous stars, broadband colours of the galaxies, and various spectroscopic indicators [170,171,172,173,174,175].

These models work well but uniqueness is a problem, especially as to determining precisely when unresolved very old stars (the ones which dominate the stellar light in most massive galaxies) form – this is because observables which are sensitive to the presence of these stars, like near-infrared colours, vary only slightly with age when the stars get old. The situation will improve significantly with the advent of the *Next Generation Space Telescope*, when we will be able to probe much further down (in terms of stellar luminosity) the colour-magnitude diagram for galaxies beyond the Local Group.

3.5 Calculation of Ω_*

Fukugita et al. (ref. 106, hereafter FHP98) sum over the optical (B-band) galaxy luminosity function to determine the luminosity density of the Universe and then compute Ω_*, the cosmological density in stars in units of the critical density. The principal uncertainties in this analysis are the normalization of the galaxy luminosity function (and

consequently the galaxy luminosity density) and the stellar initial mass function. They find

$$\Omega_* = 0.0024\, h^{-2} \left(\frac{\mathcal{L}_{\mathcal{B}}}{2.0 \times 10^8\, h\, \mathrm{L}_\odot \mathrm{Mpc}^{-3}} \right) \left(\frac{\Xi}{\Xi(\mathrm{GBF})} \right), \quad (6)$$

where $\mathcal{L}_{\mathcal{B}}$ is the local luminosity density of the Universe and Ξ(GBF) is the mass-integral of the stellar IMF appropriate to the IMF of Gould et al. [132]. About 3/4 of these stars are in spheroids (ellipticals and bulges of spirals) and 1/4 in disks. Adopting $h = 0.65$, and using the value of Ξ implicit elsewhere in this article (from Kroupa et al. [34], hereafter Ξ(KTG)), Equation (6) implies $\Omega_* = 0.0036$. The uncertainty in this value is large and depends on a number of factors:

1) Uncertainty in $\mathcal{L}_B$. This is probably about 10% of $\mathcal{L}_B$, estimated by FHP98 based on an intercomparison of the results of various redshift surveys;

2) Uncertainty in the mass integral of the stellar IMF Ξ. This is difficult to estimate because the contribution to the total stellar mass from low-mass stars is poorly determined in any galaxies other than the Milky Way. A plausible estimate of the uncertainty can be obtained by comparing the values of Ξ from different Galactic surveys: $\sigma(\Xi)/\Xi \approx [\Xi(\mathrm{KTG}) - \Xi(\mathrm{GBF})]/\Xi(\mathrm{KTG}) = 0.33$

3) Uncertainty in the global mass-to-light ratio $< \Gamma >$ averaged over all stellar populations, which can be further divided into two:

3a) Uncertainty in the conversion between mass and luminosity for a given population with known IMF. This is due to uncertainty in the models described in the previous section, which are due to uncertainties in radiation transfer modelling in stars, in modelling stellar evolution (which is sensitive to stellar ages), and in the contributions from stellar remnants of different types. It is further complicated by our lack of knowledge about the precise nature of internal extinction. FHP98 use the models of Charlot et al. [176] to determine $\Gamma = 5.4 - 8.3$ for the B-band, corresponding to a fractional uncertainty of 0.42.

3b) Uncertainty in the proportions of different stellar populations in different galaxies. For example, Simien & de Vaucouleurs [105] determine that only 61 % of the light in elliptical galaxies comes from old stars with high mass-to-light ratios, not the 100 % conventionally assumed (e. g. FHP98 and references therein). As Population II stars typically have Γ about 4 times higher than Population I stars, this uncertainty leads to a fractional uncertainty in Ω_* of about $(4 - 4 \times 0.61 - 0.39)/4 = 0.29$ for the elliptical galaxy contribution. For other galaxy types, this source of error is less, and the luminosity-weighted fractional uncertainty averaged over all galaxy types is closer to 0.2.

Combining all these uncertainties suggests a value $\Omega_* = 0.0036 \pm 0.020$.

A similar analysis done in K-band also yields $\Omega_* = 0.0036$, with comparable error. The motivation was to use data where the effects of internal extinction are small and we are able to observe the stellar populations directly. Although the method was similar, in deriving this number I tried as far as possible to use different datasets: the luminosity density was drawn from the K-band luminosity function of Szokoly et al. [177], near-infrared mass-to-light ratios from Thronson & Greenhouse [178], and near-infrared colours from de Jong [179] and Huang et al. [128]. It is therefore reassuring that the results are so similar.

In summary I conclude

$$\Omega_* = 0.0036 \pm 0.020.$$

If a Salpeter, not Kroupa et al. IMF [34] is used in deriving Ξ, a value of Ω_* a factor of two higher.

These values of Ω_* are much lower than the values of $\Omega_{\mathrm{baryon}} = 0.052 \pm 0.008\, (h/0.65)^{-2}$ inferred from big-bang nucleosynthesis (refs. 180 and 181; however note the discrepant results in the deuterium abundance derived by Songaila et al. [182] and O'Meara et al. [183]) and microwave background anisotropies [184,185]. Most of these missing baryons are not associated with galaxies at all ($\Omega_{\mathrm{gas\ in\ galaxies}} \sim 0.0006$; FHP98). Most are in ionizied gas in small groups. Theoretical arguments [186] based on the broadening of Lyα forest lines in quasar absorption spectra suggest that most baryons exist in the intergalactic medium (IGM) at $z \sim 2$. The same seems to be true at $z = 0$ although the growth of structure in the Universe between $z = 2$ and $z = 0$ means that this gas is now associated more with diffuse galaxy groups (FHP98) than in a genuine, smooth IGM.

So a picture is emerging where the mass content of the Universe [185] is about 65 % dark energy (perhaps a cosmological constant), 30 % dark matter (probably cold) which has a pressureless equation of state and clumps gravitationally, and 5 % baryons of which about one-tenth is in stars. It is interesting that this inventory, suggested mainly from observations of the cosmic microwave background in conjunction with studies of high-redshift supernovae [187], is consistent with the distribution of material in rich galaxy clusters [188]. These clusters are bound

systems that assemble at late times but represent high-σ peaks in the mass distribution, so it is likely that the star formation in the galaxies within them was complete at early times and that the cluster material distribution is close to the "end-state" distribution for the Universe. This notion is consistent with what we saw in Figure 1 – the star formation rate at the present time is very much lower than what it was in the past.

A question that follows from the previous paragraph: is the cold dark matter associated with individual galaxies containing stellar populations? Giant galaxies do not possess sufficient dark matter for this to be the case. For example, M31 has a total (including dark matter) mass-to-light ratio of about 60 [189] and a stellar mass-to-light ratio of about 5. Therefore about 1 part in 12 by mass is in stars, much higher than the ratio 0.5/30 implied in the previous paragraph. Dwarf galaxies are also not a candidate. Galaxies like Draco possess a great deal of dark matter, but not enough to explain the difference between the observed field galaxy luminosity function and the cold dark matter mass function (Figure 10). Therefore most cold dark matter is likely to reside in individual dark halos containing no stars [190] or to be smoothly distributed.

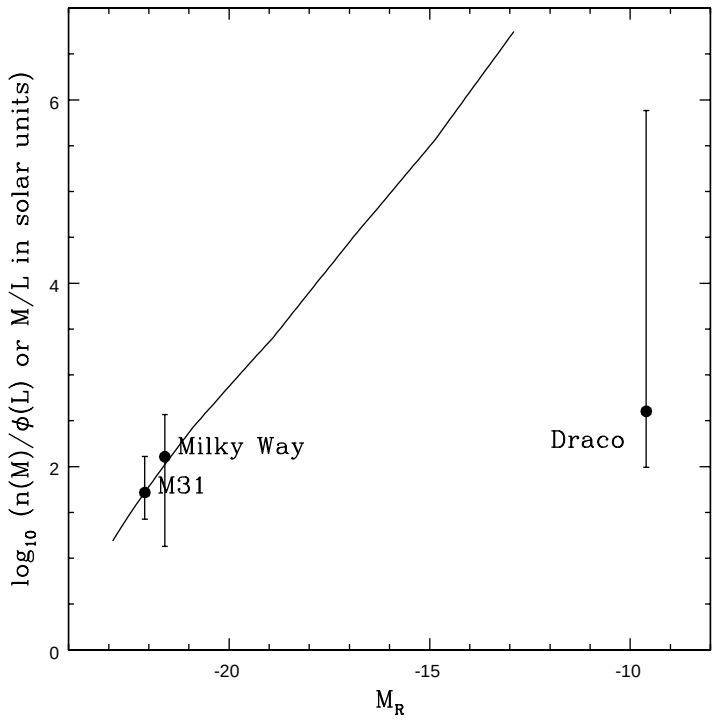

Figure 10: The ratio of the galaxy mass function to the field luminosity function, normalized so that a galaxy having $M_R = -22.1$ has a mass-to-light ratio of 60, as appopriate for M31, given the analysis of Evans & Wilkinson [189]. The mass function is computed from Press & Schechter [191] theory, assuming the CDM power spectrum of Efstathiou, Bond & White [192] with a shape parameter $\Gamma = 0.3$ and a normalization $\sigma_8 = 1$. The luminosity function is the Ursa Major luminosity function [143], assumed to be representative of the field. The three points show the mass-to-light ratios of M31 [189], the Milky Way [193] and Draco [194 with an upper limit from ref. 195], using absolute magnitude from ref. 196, adjusted to the R-band assuming $V - R = 1$.

4 THE MATCH BETWEEN THE COSMIC STAR FORMATION HISTORY AND THE LOCAL GALAXY POPULATION

A major aim of extragalactic astronomy is to combine the results of the previous two sections. The equation describing the formation of stars in the Universe is

$$\Sigma_i \int_L L\,\phi_i(L)\,\Gamma_i\,\mathrm{d}L = \int_t \mathrm{SFR}(t)\,\mathrm{d}t, \tag{7}$$

where Γ_i is the mass-to-light ratio of stellar population i (Γ_i is derived from stellar evolution and population synthesis models). Having gotten $\phi_i(L)$ and SFR(t), the aim is then to evaluate this equation in detail, matching the contributions to the sum in the first term to the relevant part of the integral in the second term. The first stage will be to evaluate the integral on the right-hand side of Equation (7); note that the sum on the left-hand side has already been computed in Section 3.5. Integration of the Madau Plot described in Section 2 gives

$$\Omega_* \approx 0.0038 \left(0.16 + 0.11 \frac{1+P_{150\,\mathrm{nm}}}{4.7} + 0.73 \frac{1+P_{280\,\mathrm{nm}}}{2.7}\right) \frac{1}{1-f_{\mathrm{IR}}}. \tag{8}$$

Here the P values are contribution-weighted averages. Given the numbers in Section 3.5, this would seem to provide evidence in favour of a small value of f_{IR}.

Below are listed some of the important observational and theoretical results that will provide constraints on the matching algorithm, along with descriptions of improvements that are expected to happen over the next few years.

4.1 Evolution of Ω_*

In an important study Papovich et al. [197] measured the evolution of Ω_* by determining the stellar masses of an optically-selected sample of field galaxies with spectroscopic or photometric redshifts. This was achieved by performing near-infrared photometry and fitting the evolutionary models described in Section 3.4 to broadband colours. Because the wavelength baseline is so long, the stellar masses are well-determined for the galaxies. A more recent study using a larger sample was performed by Dickinson et al. [198], and their results are presented in Figure 11.

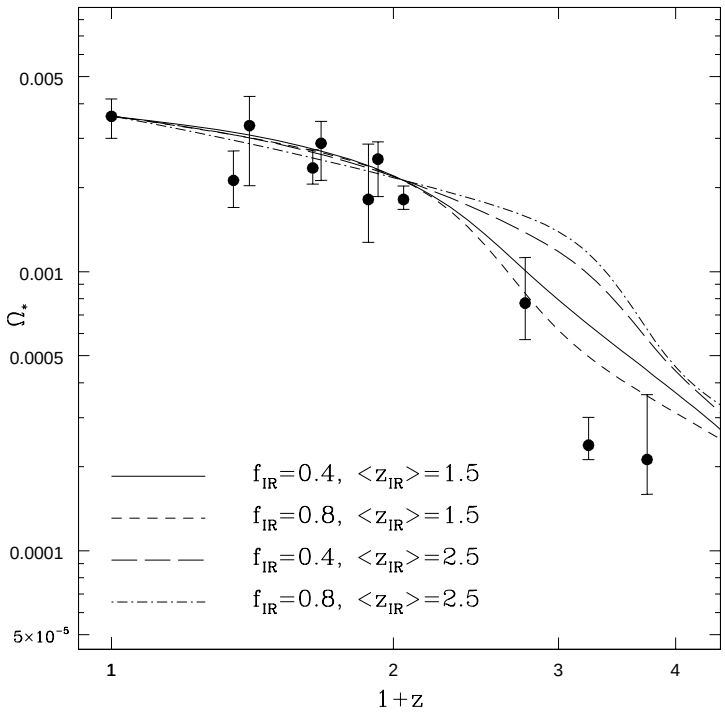

Figure 11: The evolution of Ω_* (adapted to our cosmology and stellar IMF), the cosmic density in stars. The data are from Figure 7 of Dickinson et al. [198] and come from refs. 15, 47 and 199. The lines represent the predictions of four groups of models described in Figure 4, defined by f_{IR} and $< z_{\mathrm{IR}} >$.

These studies already provide tight constraints – the error bars in Figure 11 are small. It appears that about 85% of the stars in the Universe formed between $z = 2$ and $z = 1$. Two immediate conclusions are:

1) another population of star-forming galaxies is required in addition to optical galaxies. This is because the shape of the dashed line in Figure 1 is such that its integral over time between $z = 2$ and $z = 1$, while high, does not represent 85% of the total integral. Given the discussion in Section 2, infrared galaxies would seem to be a natural candidate for this extra population;
2) the infrared Madau Plot must be heavily peaked at some redshift between $z = 2$ and $z = 1$. The four models shown in Figure 11 are all based on Gaussians in redshift with widths $\sigma_z = 0.5$, which are clearly too broad.

Since the random errors are small, one particulary constructive line of observational study will be to eliminate any possible systematic errors. The most serious systematic errors likely pertain to source selection. Much active star formation is hidden by dust and it is possible that many evolved stellar populations are also obscured by dust, particularly if dust dispersion timescales are long. These stellar populations would be missing from optical surveys. so multiwavelength selection may be required. Also surface-brightness selection effects may be important, particularly at high redshift where $(1 + z)^4$ cosmological surface-brightness dimming is important. At low redshift this is less of a concern since the systems which dominate the stellar mass in Figure 7 are high surface-brightness systems e. g. elliptical galaxies.

4.2 Stellar Population Age Matching

The construction of models describing the spectrophotometric evolution of galaxies has become an active area of research. These models are discussed in Section 3.4 and have been very successful at explaining the properties of nearby galaxies.

For higher redshift ($z > 1$) galaxies, in which much of the cosmic star formation happens, the situation is made more difficult by the fact that only broadband colours and perhaps one or two emission line diagnostics are available for each galaxy. This generally means that we can get the instantaneous star formation rate reasonably precisely, as the rest-frame blue and ultraviolet flux is heavily dominated by young, massive OB stars. If near-infrared colours are available, the total mass in stars may be determined too, as in Section 4.1. The star-formation history, however, is poorly determined for the same reason as in Section 3.4 – for all but the youngest stars (and consequently populations of stars), the models predict that broadband colours are a weak function of age.

Relative ages of populations, rather than absolute ages, are the most robust outputs of the galaxy evolution models. If we have a secure measurement of the Madau Plot, these are sufficient to fully describe the match described by Equation (7): both the left- and right-hand sides of this equation may be rewritten in differential form.

With the next generation of instruments, like those aboard the *Next Generation Space Telescope*, the match between observation and theory will improve in two ways. Firstly, we will be able to produce colour-magnitude diagrams for galaxies beyond the Local Group to faint stellar luminosities. This means that the galaxy evolution models can be tested more precisely. Secondly, observations of distant galaxies will be made at much higher signal-to-noise, allowing a more detailed comparison with the galaxy evolution models.

4.3 Chemical and gas content evolution

In general, as galaxies evolve and form more stars, their gas content decreases and their metal content increases. Later generations of stars will be more metal-rich as they will be made out of gas that is increasingly polluted. This is implicit in the models described in the previous section. Some of the metals, however, will not be retained by the galaxies and will be ejected into the IGM by stellar winds and supernovae, particularly from low-mass galaxies with small gravitational potential wells. This has a number of observational consequences.

The most direct observable signatures are the abundances in Lyα forest clouds or in the outer parts of damped Lyα systems [200,201], thought to consist of baryonic material representative of the IGM. At high redshift $z > 2.5$, the chemical compositions of the clouds [202,203,204] can now be determined e. g. using echelle spectroscopy on large telescopes. But these high redshifts do not appear (from Figure 11) to be where most cosmic star formation happens. Measurements of abundances in clouds at low redshift are difficult because they required high signal-to-noise ultraviolet spectroscopy, which can be done only with the *Hubble Space Telescope* (see e. g. the spectra in ref. 205) and even then are difficult to perform. In the future, measurements such as these will be possible with the *Next Generation Space Telescope* and will provide important constraints.

4.4 Structural Parameter Matching

If all that happens in the evolution of a galaxy is passive stellar evolution, then the density of stars within galaxies should be comparable to the gas densities in the star forming galaxies.

But secular evolution of stellar populations is important too. Processes like phase mixing and violent relaxation [206] occur in most galaxies, but do not lead to huge density changes [207], when averaged over suitably large volumes. More dramatic changes like evaporation and core collapse (following a gravothermal catastrophe) can happen, but the timescales on which these processes operate in galaxies is normally longer than a Hubble time. The presence of a massive dark halo is important too, particular as regards making galaxies stable to evaporation.

Stellar-kinematic mergers also play an important role in determining the final stellar densities. These are considered separately in the next section.

Apart from studies of mergers, progress will be made in following areas;

1) integral field units on large telescopes will permit spatially resolved spectroscopy of star-forming galaxies. This will permit us to determine the conditions at the precise locations where most of the star formation is happening in these galaxies. This will be particularly important at near-infrared wavelengths [208] since we may be able to make measurements in infrared galaxies like the host of GRB 980703, at least in the ones that are not too heavily obscured. Additionally measurements of optical galaxies will be possible, allowing a determination of R;

2) as millimetre line receivers become more sensitive and as the number of infrared galaxies known increases, studies of different transitions of different molecular species in the infrared galaxies will become possible. Given the discussion in Section 2.5, it might be expected that species like HCN and CS, which probe extremely high densities, will not be detected in the bulk of infrared galaxies, so a significant number of positive detections would imply that $f_{\rm IR}$ is low;

3) as spectrographs get more sensitive and are used on increasingly large telescopes, absorption-line studies will become possible on increasingly distant evolved stellar populations. Constraints will come from such studies, when performed on galaxies in the samples used in Section 4.1. There will be two types of constraints;

3a) direct measurements of the kinematic of stars in high-redshift galaxies, and

3b) very-high signal-to-noise measurements of the kinematics of stars in intermediate-redshift ($0.1 < z < 1$) galaxies, like has already been done for a few $z = 0$ elliptical galaxies and bulges [209]. A template sample can then be constructed, and the kinematics of stars in high-redshift galaxies determined by matching to this template sample if the signal-to-noise of the high-redshift galaxy spectra is low, perhaps with the help of non-spectroscopic indicators like colours and morphologies.

4.5 Mergers

Galaxy mergers not only affect the galaxy luminosity by redistributing light to systems of higher luminosity (with or without triggering new star formation), but also the density structure of galaxies. In particular stars found at very low densities could have been ejected as debris from higher-density regions during galaxy mergers, perhaps following the formation of tidal tails (e. g. ref. 210). These stars may fall back onto the remnant galaxy or they may become unbound, depending on the ejection velocity and the parent galaxy masses.

The reason galaxy mergers happen is normally due to the collisions of dark matter halos as structure builds up on large mass scales in hierarchical galaxy formation scenarios like cold dark matter theory. The halos drag their associated baryons, which we observe as galaxies, with them, and the result is a galaxy merger. Galaxy mergers often have spectacular morphologies.

In summary, the final density structure of galaxies is determined by the joint effects of the (gas) density at which the stars form, secular evolution, and the redistribution of stars in stellar kinematic mergers. Mergers are quite possibly the most important of the three, as they can lead to fairly dramatic changes in the late stages of galaxy evolution.

Particular areas where the study of mergers is evolving rapidly are:

1) observations of high-redshift mergers. Larger optical telescopes mean improved improved imaging capability in the outer parts of interacting galaxies where dynamical clocks run slowest, the merger signature is strongest, but the signal-to-noise is low;

2) studies of low-redshift mergers. This is driven by (1) increased sensitivity in submillimetre and millimetre line and continuum (as well as optical) imaging, and (2) increased computer power. Detailed numerical modelling of a

large sample of local mergers, each observed to a high level of precision, will provide an important template that can be compared to high-redshift galaxies, for which only limited measurements are available;

3) determination of the evolution of the luminosity function of evolved stellar populations, identified as in Section 4.1. This should provide a reasonably direct measurement of the evolution of the merger rate, so long as contributions from newly-formed stars are removed. Perhaps this will be difficult if the fraction of mergers at high-redshift that are predominantly stellar-kinematic and involve no new star formation is small. If so, this will be important to know;

4) measurement of the optical intergalactic light, that which contributes to the EBL but is outside galaxies. Techniques [102] are already in place to do this. If it is assumed that the majority of stars seen between galaxies were flung out and became unbound during mergers, this measurement provides a constraint on the integrated (over time) merger rate. If optical colours of this intergalactic light can also be measure this provides (in conjunction with the galaxy evolution models) a constraint on the redshift-dependance on the merger rate. A possible source of contamination which needs to be subtracted from this measurement is the contribution from galaxies that are not resolved because their surface brightnesses are too low. These are mainly low-luminosity galaxies, and most current indications (e. g. ref. 16) are that this contribution is small.

4.6 Joint Magorrian Relation Considerations

An identical analysis can be performed for the formation of supermassive black holes in the centres of galaxies, many of which also seem to form in a dust-enshrouded phase (e. g. ref. 211). This process and the formation of stars must happen in such a way so as to produce at the end the tight correlations observed between stellar mass and black hole mass (e. g. ref. 39). The joint consideration of star formation histories and supermassive black holes formation histories will provide constraints on the mapping described by Equation (7). It is worth discussing two extreme scenarios.

One possible scenario is that most of the mass build-up in AGNs happens during mergers of two massive galaxies. This is essentially the scenario proposed by Sanders et al. [37,38] and described at the end of Section 2.5. The evidence on which this scenario is based is that the timescales for the build-up of mass in supermassive black holes are short [e. g. ref. 212] and that the host galaxies of *all* AGNs observed (these are all at $z < 0.5$) are massive systems. This is true all along the evolutionary sequence described in Section 2.5: both for ULIGs that are probably AGN-powered (e. g. Markarian 231) and for optical quasars (e. g. 3C 273). As AGNs evolve along the sequence, their AGNs heat and then disrupt their dust shrouds so that the most evolved luminous AGNs (radio-loud quasars [212]) reside in the most dynamically evolved stellar systems (e.g. elliptical galaxies; ref. 213). The problem with this scenario is that most star formation appears to happen between $z = 2$ and $z = 1$, whereas the quasar luminosity density redshift distribution peaks at $z > 2$ [214], yet quasars are expected to happen in the very latest stages of AGN evolution.

A second possible scenario is that most of the mass build-up in AGNs happens during the early stages of galaxy assembly, before most stars formed. The systems which later merged to form spheroids would already contain black holes at the time of the merger. The Magorrian relation is then set by two physical processes: 1) spheroids are made during mergers [215] via physical processes like violent relaxation so that the Magorrian relation applies to spheroids specifically and not disks [216], and 2) the proportion of gas ending up in the central black hole in the final object is set by the proportion of gas within a catchment volume that is capable of collapsing to very small radii within one of the bound sub-units within the volume. This proportion depends on small-scale physical effects and is unlikely to vary significantly from one catchment volume to another, since the volumes we need to average over to determine these proportions are so big. When the subsystems merge in this context, the stellar remnant (an elliptical or spiral bulge) may then possess a binary black hole, depending on the details of this merger. Such a binary system is observed in both M31 [217] and NGC 6240 [218], although the binary in NGC 6240, a rapidly evolving galaxy, may eventually merge to form a single black hole. The main problem with this scenario is that no local examples of galaxies with massive black holes but few stars are known. All local AGNs, including low-luminosity ones, are in massive galaxies and these would in this context all be secondary accretion events. For this scenario to remain viable, we would need considerable fine tuning: the entire process of gas collapse in subunits within a catchment volume plus AGN build-up cannot be too efficient a process or the AGN luminosity density distribution [214] would peak at much higher redshifts or too inefficient a process or we would see at least some local examples.

Maybe both scenarios are operating at some level. In either case, a seed black hole [219] may be required to trigger the entire process.

The observational tests required here are conceptually simple: deep imaging of the host galaxies of powerful AGNs is required. Paricularly important are measurements of AGNs at different evolutionary stages, perhaps identified by their SEDs. If the first scenario is correct, host galaxies of AGNs at all evolutionary stages will be massive, evolved stellar systems and will show signs of tidal debris in their outer parts (where dynamical clocks run slowest), even if they look like elliptical galaxies in their centres. The morphologies of the host galaxies will become progressively more relaxed as the AGNs grow. If the second scenario is correct, host galaxies of AGNs at all evolutionary stages (other than secondary accretion events) will be gas-rich galaxies yet to form their stars. The existing stellar content of these systems will be small.

The constraints will improve in the future but already they are good enough to provide perhaps the strongest constraint on a *low* value of $f_{\rm IR}$. Most galaxies that contribute to the infrared Madau plot have redshifts $2 > z > 1$ (see Section 4.1). Yet these are the galaxies which are most likely to evolve into dense (Section 2.5) spheroidal (Section 3.5) stellar systems, the ones that harbour black holes. It is the less dense optical galaxies that dominate the Madau Plot at high redshift, but the most luminous AGNs appear to be in place by then. Considerable fine tuning is then required to maintain a high $f_{\rm IR}$, which is what is suggested by many of the other observations discussed in Section 2.

4.7 Number Counts

Galaxies have SEDs characterized by L_ν, which are directly related to fluxes f_ν or apparent magnitudes $m_\nu = -2.5 \log_{10} f_\nu$ + constant.

For any model of the galaxy population evolution, at each time or redshift each galaxy is characterized by a particular SED. Summing over the entire galaxy population,

$$n(f_\nu) = \int_V \int_{\frac{4\pi d_L(z)^2 f_\nu}{(1+z)}} \phi(L_\nu, z)\, {\rm d}L_\nu\, {\rm d}V(z), \tag{9}$$

where fluxes f_ν are related to magnitudes m_ν as above. Here $\phi(L_\nu, z)$ is the redshift-dependent luminosity-density function: the SED L_ν is related to the bolometric luminosity L by $L = \int_0^\infty L_\nu\, {\rm d}\nu$ and the luminosity in any passband T defined by the transmission function $T(\nu)$ as $L_T = \int_0^\infty L_\nu\, T(\nu)\, {\rm d}\nu / \int_0^\infty T(\nu)\, {\rm d}\nu$. This must be consistent with optical [220] and near-infrared [221,222,223] number count data.

Normally the number counts are presented as binned data, where the number of galaxies in each bin is determined over a large surface area of sky (so that uncertainties due to cosmic variance are small). The reasons a particular galaxy at a given redshift may leave or enter a bin are

1) the turning on of star formation in a galaxy. This is normally a large effect. If an infrared galaxy, the galaxy can move up several bins for all T in the infrared. If an optical galaxy, the galaxy can move up (i. e. brightward) several bins for all T in the ultraviolet or optical, unless it already has a substantial existing stellar population (e. g. star formation that is suddenly turned on in local early-type or Sa galaxies), in which case it only moves up a small number of bins;

2) stellar redistribution by mergers. If two galaxies merge and the merger is purely stellar-kinematic and not accompanied by new star formation, they both disappear from their existing bins and reappear as a single unit is a higher bin. This is normally a moderate effect, corresponding to a bin shift of about 1 magnitude for an equal-mass merger. The shift happens everywhere in the spectrum but is generally most important at optical wavelengths, since this is where the SEDs of existing stellar populations peak. Conversely, if a galaxy is broken into several smaller galaxies e. g. by a collision, a single unit in a high-flux bin will reappear as several smaller units in low-flux bins;

3) as the stellar populations in galaxies evolve, they normally do so in the sense of decreasing L (fading) and a shift in L_ν towards longer wavelengths (lower frequencies). For such passively-evolving galaxies, there is therefore a slow migration towards bins of fainter flux and decreasing frequency;

4) as dust in a galaxy clumps, disperses, or gets destroyed, more light becomes visible at ultraviolet and optical wavelengths and the SED changes to reflect this. This leads further to a trend of increasing $n(m_\nu)$ towards lower frequencies. This is particularly important if infrared galaxies at high redshift evolve into (relatively) gas-poor stellar populations at low redshift;

5) if AGN activity is turned on, a galaxy can move upward by several bins. Where in wavelength space this is most important depends on the SED of the AGN (see Section 2.5), which in turn depends on its evolutionary state. In principle this could affect number counts everywhere from the radio to the X-ray, particularly at the highest flux levels. However, AGNs are unlikely to affect the bulk of the number counts since their contribution to the EBL is small (see Section 2.2).

4.8 The Milky Way Galaxy

Historically measurements of stars within the Milky Way galaxy have provided the most rigorous constraints on its formation [224]. Over the next few years these measurements will increase in precision and stellar sample sizes will become much bigger.

Clearly our knowledge of the formation of the Milky Way will expand. The application to the wider galaxy formation problem is less clear to assess at this stage, but it seems a good idea to look for similarities between the Milky Way and field galaxies at all redshifts, as far as possible. This may well become a major observational industry over the next few years, as many more measurements of stars within the Milky Way are made. Both photometric and spectroscopic indicators will be useful. Presumably the level of significance of all measurements will decrease with increasing distance so such a procedure will, no doubt, be piecemeal.

5 SUMMARY

The formation of stars in galaxies is a well-defined problem and detailed solutions will come from observational studies and modelling. The progress currently being made in both areas is rapid, but some results are more secure than others in terms of their applicability to the overall problem. The aim of the current article is to place the results in this context.

Our current knowledge of even the basic form of the Madau Plot is poor because the redshift distribution of the infrared Madau Plot is unknown. In fact, even the value of $f_{\rm IR}$ is unknown, although various measurements, like the SCUBA 850-μm counts and the radio detections of optically-faint GRB host galaxies, lead us to suspect that it is high.

Conversely the galaxy luminosity function at $z = 0$ is now very well determined. The normalization is well known from the large number of big redshift surveys currently in progress and the extreme faint end is known from deep surveys of nearby diffuse groups of galaxies carried out using large-format mosaic CCDs on 8 m telescopes.

Modelling of astrophysical processes like mergers and star formation in galaxies is rapidly becoming more detailed because 1) increased computer power allows simulations with larger numbers of particles and/or resolution elements, and 2) the observational constraints on models are becoming tighter as new discoveries are made and the signal-to-noise of existing observational results increases. This is similarly true of the stellar population evolutioon models described in Section 3.4.

Extragalactic astronomy is therefore a technologically-driven field and much progress will happen over the next few years.

Many of the formalisms required to match the Madau Plot to the local galaxy function have already been developed, as part of semi-analytic galaxy formation models [225]. Conceptually semi-analytic models [23,226,227] adopt quite a different approach to that described here. They follow the gravitational growth of dark matter perturbations and the collapse of baryons within them and attempt to model the large number of physical processes that operate as this gas is converted into stars. The end product is the information listed in Section 3, and the Madau Plot is output along the way. Here we start with the Madau Plot, and deal with the various physical processes in a purely empirical way, so are in effect only concerned with a limited part of the galaxy formation process. The semi-analytic models, on the other hand, directly use recipes constructed from the laws of physics. This approach has the advantage of putting the entire galaxy formation process on a firm footing as regards the laws of physics. It has the disadvantage that many of the more important physical processes, particularly feedback during star formation [228], are so poorly constrained by observation that detailed modelling is not rigorous. As the observational issues highlighted in this article get resolved, detailed modelling of the physics is a natural next step.

ACKNOWLEDGEMENTS

Figures 2 and 3 are reprinted from Physics Reports, Vol. 369, p. 111-176 "Submillimeter Galaxies" by Blain et al., Copyright (2002) with permission from Elsevier.
Discussions with my colleagues Andrew Blain, Aaron Evans, Jeff Goldader, Simon Hodgkin, Tae Sun Kim, Priya Natarajan, Bianca Poggianti, Enrico Ramirez-Ruiz, Martin Rees, Dave Sanders, Brent Tully, and Mark Wilkinson are gratefully acknowledged. Also I thank Richard Sword for making Figure 9 and Shireen Mohandes for helping to prepare the manuscript.

ADDENDUM

In the few weeks since this article was submitted for publication, a number of recent results have appeared in the literature that are relevant to this work. Three studies in particular are important in the context of this review.

(i) A median redshift of 2.4 for galaxies bright at submillimetre wavelengths – Chapman et al. 2003, Nature

Using the techniques outlined in Section 2.4.1.1, Chapman et al. [A1] have identified and measured the redshifts of a sample of 10 submillimetre sources. They find a median redshift of 2.4.

This is somewhat higher than the redshift of the bulk of cosmic star formation required by the studies described in Section 4.1. This could be reconciled with a high $f_{\rm IR}$ and submillimetre background if the bulk of the sources which dominate the submillimetre background, the $S_{850} = 1$ mJy sources, lie at lower redshifts than the sources Chapman et al. observed. There is some evidence for this (see Fig. A1). Interestingly, the two lowest-redshift sources of have dust temperatures of only 16 K and 25 K, and consequently low star-formation rates. If these are typical of infrared star-forming galaxies, then $f_{\rm IR}$ may be reasonably low even if the submillimetre background is high.

On the other hand, the lower-flux submillimetre sources may have a similar redshift distribution to their higher-flux counterparts. This could be reconciled with Figure (11) if either

1) the Chapman et al. sample is contaminated by dust-enshroouded AGNs. This is suggested by the warm dust temperatures of the more energetic sources in the sample and the concordance between the redshifts of the SCUBA sources and of high-redshift quasars [214,A2]

2) the SCUBA sources are forming stars that are later cannibalized by an AGN. Each parcel of hydrogen is then responsible for creating two sets of photons: one set when hydrogen is converted to helium in stars, and one set when stellar mass is converted to black hole mass as the AGN grows. This scenario has the advantage of generating a low Ω_* and local supermassive black hole mass density while maintaining a large $I_{\rm opt}$ and $I_{\rm IR}$, all of which are supported by observation.

(ii) Bimodality in the Clustering Properties – Budavari et al. 2003, ApJ

Using photometric redshifts for a very large (2 million) sample of galaxies from the Sloan Digital Sky Survey, Budavari et al. [A3] noticed strong bimodality of clustering properties when the galaxies were segregated by spectral type. Evolved red galaxies have been known for some time to cluster more strongly than star-forming galaxies but the new data shows that the transition between the two regimes is very abrupt – somewhat evolved, moderately red galaxies cluster strongly like very evolved, very red galaxies, and moderately blue galaxies cluster weakly like actively star-forming galaxies that are very blue.

These results point towards two distinct formation environments for galaxies. It may follow from this that there could exist two possible types of global mechanism for converting gas into stars in galaxies – perhaps this could lead to two types of star forming galaxy: optical and infrared.

Following the evolution of the spectral-type subsamples defined by Budavari et al. will give a strong constraint on the match defined by Equation (7). Tracking the galaxies backward in time allows us to estimate when their stars formed out of gas and where on the Madau plot they lie. Tracking them forward in time tells us which stellar populations in the local Universe they correspond to and therefore their contribution to the local luminosity function. This constraint on the match defined by Equation (7) is a very indirect one, but the significance of the bimodality measured by Budavari et al. is high enough that it will probably be an important complement to the measurements desribed in Section 4.

Figure A1: The redshifts and star-formation (or AGN mass-accretion) rates for the SCUBA samples of Chapman et al. (ref. A1) and the hosts of the four GRBs described in Section 2.4 that are infrared galaxies.

(iii) Hα Spectroscopy of Galaxies at $z > 2$ – Erb et al. 2003, ApJ

This work [A4] presents evidence that star-formation rate derived from nebular abundances is somewhat higher relative to the star-formation rate derived from broadband luminosities at $z = 2$ than it is at $z = 3$.

The redshift dependence of this effect appears to be moderated through the galaxy luminosity. The $z \sim 2$ galaxies studied by Erb et al. have lower total luminosity and star-formation rate than the $z \sim 3$ galaxies studied by Pettini et al. [53]

If both samples of galaxies are typical of the ones which dominate the cosmic star formation at the relevent epoch, there are important implications for how we determine the P values in Equation (8) – these are redshift-averaged values weighted by the cosmic star-formation happening at each redshift. Specifically $P_{280\,\mathrm{nm}}$ may be higher relative to $P_{150\,\mathrm{nm}}$ than we might expect from simple application of a Galactic extinction law. The third term in the parentheses in Equation (8) then contributes more relative to the second term than we might expect and consequently the argument made in Point 1) in Section 4.1 is weakened. Indeed the considerable reradiated flux in the $z \sim 2$ galaxies studied by Erb et al. may be enough to turn these optical galaxies into the very galaxies postulated to exist there.

However, the Erb et al. sample is small and therefore this kind of assertion should be made with caution at this stage.

References

[1] Blumenthal G. R., Faber S. M., Primack J. R., Rees M. J., 1984, Nature, 311, 517
[2] Bardeen J. M., Bond J. R., Kaiser N., Szalay A. S., 1986, ApJ, 304, 15
[3] White S. D. M., Rees M. J., 1978, MNRAS, 183, 341

[4] Madau P., Ferguson H. C., Dickinson M. E., Giavalisco M., Steidel C. C., Fruchter A., 1996, MNRAS, 283, 1388
[5] Hauser M. G. et al., 1998, ApJ, 508, 25
[6] Schlegel D. J., Finkbeiner D. P., Davis M., 1998, ApJ, 500, 525
[7] Fixsen D. J. et al., 1998, ApJ, 508, 123
[8] Smail I., Ivison R. J., Blain A. W., 1997, ApJ, 490, L5
[9] Berger E., Kulkarni S. R., Frail D. A., 2001, ApJ, 560, 652
[10] Berger E., Cowie L. L., Kulkarni S. R., Frail D. A., Aussel H., Barger A. J., 2003, ApJ, submitted (astro-ph/0210645)
[11] Frail D. A. et al., 2002, ApJ, 565, 829
[12] Schechter P. L., 1976, ApJ, 203, 297
[13] Binggeli B., Sandage A., Tammann G. A., 1988, ARA&A, 26, 509
[14] Blanton M. R. et al., 2001, AJ, 121, 2358
[15] Cole S. et al., 2001, MNRAS, 326, 255
[16] Trentham N., Tully R. B., 2002, MNRAS, 335, 712
[17] Alcock C. et al., 2000, ApJ, 542, 281
[18] Oppenheimer B. R., Hambly N. C., Digby A. P., Hodgkin S. T., Saumon D., 2001, Science, 292, 698
[19] Fields B. D., Freese K., Graf D. S., 1998, New Astron, 3, 347
[20] Carroll S. M., Press W. H., Turner E. L., 1992, ARAA, 30, 499
[21] Lilly S. J., Le Fèvre O., Hammer F., Crampton D., 1996, ApJ, 460, L1
[22] Efstathiou G., Bridle S. L., Lasenby A. N., Hobson M. P., Ellis R. S., 1999, MNRAS, 303, L47
[23] Somerville R. S, Primack J. R., Faber S. M., 2001, MNRAS, 320, 504
[24] Leitherer C., Heckman T. M., 1995, ApJS, 96, 9
[25] Smail I., Ivison R. J., Blain A. W., Kneib J.-P., 2002, MNRAS, 331, 495
[26] Chapman S. et al., 2000, MNRAS, 319, 318
[27] Ivison R., Smail I., Le Borgne J.-F., Blain A. W., Kneib J.-P., Bezecourt J., Kerr T. H., Davies J. K., 1998, MNRAS, 298, 583
[28] de Jong T., Clegg P. E., Soifer B. T., Rowan-Robinson M., Habing H. J., Aumann H. H., Raimond E., 1984, ApJ, 278, L67
[29] Djorgovski S. et al., 1998, ApJ, 508, L17
[30] Ramirez-Ruiz E., Trentham N., Blain A. W., 2002, MNRAS, 329, 465
[31] Blain A. W., Kneib J.-P., Ivison R. J., Smail I., 1999, ApJ, 512, L87
[32] Blain A. W., Smail I., Ivison R. J., Kneib J.-P., 1999, MNRAS, 302, 632
[33] Blain A. W. 2001, in Tacconi T., Lutz D. eds., Starburst Galaxies: Near and Far. Springer, Berlin, p 303
[34] Kroupa P., Tout C. A., Gilmore G., 1993, MNRAS, 262, 545
[35] Madau P., Pozzetti L., 2000, MNRAS, 312, L9
[36] Pozzetti L., Madau P., Zamorani G., Ferguson H. C., Bruzual A. G., 1998, MNRAS, 298, 1133
[37] Sanders D. B., Soifer B. T., Elias J. H., Madore B. F., Matthews K., Neugebauer G., Scoville N. Z., 1988, ApJ, 325, 74
[38] Sanders D. B., Soifer B. T., Elias J. H., Neugebauer G., Matthews K., 1988, ApJ, 328, L35
[39] Magorrian J. et al., 1998, AJ, 115, 2285
[40] Blain A. W., Smail I., Ivison R. J., Kneib J.-P., Frayer D. T., 2002, Physics Reports, 369, 111
[41] Gallego J., Zamorano J., Aragon-Salamanca A., Rego M., 1995, ApJ, 455, L1
[42] Tresse L., Maddox S. J., Le Fèvre O., Cuby J.-G., 2002, MNRAS, 337, 369
[43] Gallego J., García-Dabó C. E., Zamorano J., Aragón-Salamanca A., Rego M., 2002, ApJ, 570, L1
[44] Hicks E. K. S., Malkan M. A., Teplitz H. L., McCarthy P. J., Yan L., 2002, ApJ, 581, 205
[45] Cowie L. L., Songaila A., Barger A. J., 1999, AJ, 118, 603
[46] Connolly A. J., Szalay A. S., Dickinson M., Subbarao M. U., Brunner R. J., 1997, ApJ, 486, L11
[47] Cohen J. G., 2002, ApJ, 567, 672
[48] Steidel C. C., Giavalisco M., Pettini M., Dickinson M., Adelberger K. L., 1996, ApJ, 462, L17
[49] Steidel C. C., Adelberger K. L., Giavalisco M., Dickinson M., Pettini M., 1999, ApJ, 519, 1
[50] Flores H., Hammer F., Thuan T. X., Césarsky C., Desert F. X., Omont A., Lilly S. J., Eales S., Crampton D., Le Fèvre O., 1999, ApJ, 1, 148
[51] Mathis J. S., 1990, ARA&A, 28, 37

[52] Calzetti D., 1997, AJ, 113, 162
[53] Pettini M., Shapley A. E., Steidel C. C., Cuby J.-G., Dickinson M., Moorwood A. F. W., Adelberger K. L., Giavalisco M., 2001, ApJ, 554, 981
[54] Weynmann R.J., Stern D., Bunker A., Spinrad H., Chaffee F. H., Thompson R. L., Storrie-Lombardi L. J., 1998, ApJ, 505, L95
[55] Spinrad H., Stern D., Bunker A., Dey A., Lanzetta K., Yahil A., Pascarelle S., Fernández-Soto A., 1998, AJ, 116, 2617
[56] Hu E. M., Cowie L. L., McMahon R. G., 1998, ApJ, 502, L99
[57] Hu E. M., Cowie L. L., McMahon R. G., Capak P., Iwamuro F., Kneib J.-P., Maihara T., Motohara K., 2002, ApJ, 568, L75
[58] Lanzetta K. M., Yahata N., Pascarelle S., Chen H. -W., Fernández-Soto A., 2002, ApJ, 570, 492
[59] Sanders D. B., Mirabel I. F., 1996, ARA&A, 34, 749
[60] Trentham N., 2001, MNRAS, 323, 542
[61] Kaviani A., Haehnelt M. G., Kauffmann G., 2002, MNRAS submitted (astro-ph/0207238)
[62] Papadopoulos P., Ivison R., Carilli C., Lewis G., 2001, Nature, 409, 58
[63] Holland W. S. et al., 1999, MNRAS, 303, 659
[64] Blain A. W., Ivison R. J., Smail I., 1998, MNRAS, 296, L29
[65] Barger A. J., Cowie L. L., Sanders D. B., 1999, 518, L5
[66] Wilner D. J., Wright M. C. H., 1997, ApJ, 488, L67
[67] Trentham N., Blain A. W., Goldader J., 1999, MNRAS, 305, 61
[68] Smail I., Ivison R. J., Kneib J.-P., Cowie L. L., Blain A. W., Barger A. J., Owen F. N., Morrison G., 1999, MNRAS, 308, 1061
[69] Gear W. K., Lilly S. J., Stevens J. A., Clements D. L., Webb T. M., Eales S. A., Dunne L., 2000, 316, L51
[70] Dey A., Graham J. R., Ivison R. J., Smail I., Wright G. S., Liu M. C., 1999, ApJ, 519, 610
[71] Dunne L., Clements D. L., Eales S. A., 2000, MNRAS, 319, 813
[72] Yun M. S., Carilli C. L., 2002, ApJ, 568, 88
[73] Ivison R. J. et al., 2002, MNRAS, 337, 11
[74] sirtf.caltech.edu/SSC/obs/overview.html
[75] van Paradijs J., Kouveliotou C., Wijers R. A. M. J., 2000, ARA&A, 38, 379
[76] MacFadyen A., Woosley S., Heger A., 2001, ApJ, 550, 410
[77] Piro L. et al., 2000, Science, 290, 955
[78] Amati L. et al., 2000, Science, 290, 953
[79] Bloom J. S. et al. 1999, Nature, 401, 453
[80] http://www.mpe.mpg.de/ %7ejcg/grbgen.html)
[81] Sethi S., Bhargavi S. G., 2001, A&A, 376, 10
[82] Waxman E., Draine B. T., 2000, ApJ, 537, 796
[83] Galama T. J., Wijers R. A. M. J., 2001, ApJ, 49, L209
[84] Venemans B. P., Blain A. W., 2001, MNRAS, 325, 1777
[85] Fruchter A. S., Krolik H. J., Rhoads J., 2001, ApJ, 563, 597
[86] Sakamoto K., Scoville N. Z., Yun M. S., Crosas M., Genzel R., Tacconi L. J., 1999, ApJ, 514, 68
[87] Djorgovski S. G., Frail D. A., Kulkarni S. R., Bloom J. S., Odewahn S. C., Diercks A., 2001, ApJ, 562, 654
[88] Gorosabel J. et al., 2003, A&A, in press (astro-ph/0212334)
[89] Elvis M., Wilkes B. J., McDowell J. C., Green R. F., Bechtold J., Willner S. P., Oey M. S., Polomski E., Cutri R., 1994, ApJS, 95, 1
[90] Tran Q. D., Lutz D., Genzel R., Rigopolou D., Spoon H. W. W., Sturm E., Gerin M., Hines D. C., Morwood A. F. M., Sanders D. B., Scoville N., Taniguchi Y., Ward M., 2001, ApJ, 552, 527
[91] McMahon R. G., Priddey R. S., Omont A., Snellen I., Withington S., 1999, MNRAS, 309, L1
[92] Knudsen K. K., van der Werf P., Jaffe W., 2001, in Lowenthal J., Hughes D. H., eds, Deep submillimeter surveys: implications for galaxy formation and evolution, World Scientific, Singapore, p. 168
[93] Farrah D., Serjeant S., Efstathiou A., Rowan-Robinson M., Verma A., 2002, MNRAS, 335, 1163
[94] Rowan-Robinson M., Efstathiou A., 1993, MNRAS, 263, 675
[95] Saunders W., Rowan-Robinson M., Lawrence A., Efstathiou G., Kaiser N., Ellis R. S., Frenk C. S., 1990, MNRAS, 242, 318

[96] Péroux C., McMahon R. G., Storrie-Lombardi L. J., Irwin M. J., 2001, MNRAS, submitted (astro-ph/0107045)
[97] Lu L., Sargent W. L. W., Barlow T. A., Churchill C. W., Vogt S. S., 1996, ApJS, 107, 475
[98] Rowan-Robinson M. et al., 1997, MNRAS, 289, 490
[99] Kennicutt R. C., 1998, ARA&A, 36, 189
[100] Blain A. W., Jameson A., Smail I., Longair M. S., Kneib J.-P., Ivison R. J., 1999c, MNRAS, 309, 715
[101] Lagache G., Abergel A., Boulanger F., Desert F.-X., Puget J.-L., 1999, A&A, 344, 322
[102] Bernstein R. A., Freedman W. L., Madore B. F., 2002, ApJ, 571, 56
[103]) Kormendy J., 1977, ApJ, 217, 406
[104] Kent S. M., 1985, ApJS, 59, 115
[105] Simien F., de Vaucouleurs G., 1986, 302, 564
[106] Fukugita M., Hogan C. J., Peebles P. J. E., 1998, ApJ, 1998, 503, 518
[107] Toomre A., Toomre J., 1972, ApJ, 178, 623
[108] Bothun G. D., Impey C. D., Malin D. F., Mould J. R., 1987, AJ, 94, 23
[109] Freeman K., Bland-Hawthorn J., 2002, AR&A, 40, 487
[110] Binney J., Merrifield M., 1997, Galactic Astronomy, Princeton University Press Princeton
[111] Odenkirchen M. et al., 2001, ApJ, 548, L165
[112] Hodgkin S. T., Oppenheimer B. R., Hambly N. C., Jameson R. F., Smartt S. J., Steele I. A., 2000, Nature, 403, 57
[113] Reid I. N., Sahu K. C., Hawley S. L., 2001, ApJ, 559, 942
[114] Koopmans L. V. E., Blandford R. D., 2001, in Natarajan P., ed., The Shapes of Galaxies and their Halos, in press (astro-ph/0106392)
[115] Hansen B. M. S., 2003, ApJ, 582, 915
[116] Alcock C. et al., 2000, ApJ, 542, 281
[117] Hansen B. M. S., 1999, ApJ, 517, L39
[118] Lynden-Bell D., Tout C. A., 2001, ApJ, 558, 1
[119] Gilmore G., 1999, in Spooner N. J. C., Kudryatsev V., eds., The Implications of Dark Matter. World Scientific, Singapore, p. 121
[120] Alam J.-E., Raha S., Sinha B., 1999, ApJ, 513, 572
[121] Derue F. et al., 1999, A&A, 351, 87
[122] Loveday J., Peterson B. A., Efstathiou G., Maddox S. J., 1992, ApJ, 390, 338
[123] Cowie L. L., Songaila A., Hu E. M., Cohen J. G., 1996, AJ, 112, 839
[124] Ellis R. S., Colless M., Broadhurst T., Heyl J., Glazebrook K., 1996, MNRAS, 280, 235
[125] Lin H., Kirshner R. P., Shectman S. A., Landy S. D., Oemler A., Tucker D. L., Schechter P. L., 1996, ApJ, 464, 60
[126] Norberg P. et al. 2002, MNRAS, 336, 907
[127] Marzke R., Geller M. J., Huchra J. P., Corwin H. G., 1994, AJ, 108, 437
[128] Huang J.-S., Cowie L. L., Luppino G. A., 1998, ApJ, 496, 31
[129] Gilmore G., Howell D., 1998, The Stellar Initial Mass Function. ASP, San Francisco
[130] Salpeter E. E., 1955, ApJ, 121, 161
[131] Scalo J. M., 1986, Fundam. Cosmic Phys., 11, 1
[132] Gould A., Bahcall J. N., Flynn C., 1996, ApJ, 465, 759
[133] van der Marel R. P., 1991, MNRAS, 253, 710
[134] Faber S. M., 1973, ApJ, 179, 731
[135] Kormendy J., 1990, in Kron R. G., ed., The Edwin Hubble Centennial Symposium: The Evolution of the Universe of Galaxies. Astronomical Society of the Pacific, San Francisco, p. 33
[136] Carter D., Inglis I., Ellis R. S., Efstathiou G., Godwin J. G., 1985, MNRAS, 212, 471
[137] Disney M. J., 1976, Nature, 263, 573
[138] Binggeli B., 1994, in Meylan G., Prugneil P., ed., ESO Conference and Workshop Proceedings No. 49: Dwarf Galaxies. European Space Observatory, Munich, p. 13
[139] Wilkinson M. I., Kleyna J., Evans N. W., Gilmore G., 2002, MNRAS, 330, 778
[140] Armandroff T. E., da Costa G., 1999, in Whitelock P., Cannon R., ed., IAU Symposium 192: The stellar content of Local Group galaxies. ASP, San Francisco, p. 203
[141] Whiting A. B., Hau G. K. T., Irwin M. J., 1999, AJ, 118, 2767

[142] Tully R. B., Verheijen M. A. W., Pierce M. J., Huang J.-S., Wainscoat R. J., 1996, AJ, 112, 2471
[143] Trentham N., Tully R. B., Verheijen M. A. W, 2001, MNRAS, 325, 385
[144] Trentham N., Hodgkin S., 2002, MNRAS, 333, 423
[145] Tully R. B., Somerville R. S., Trentham N., Verheijen M. A. W., 2002, ApJ, 569, 573
[146] Benson A. J., Frenk C. S., Baugh C. M., Cole S., Lacey C. G., 2002, MNRAS, submitted (astro-ph/0210354)
[147] Kormendy J., Djorgovski S., 1989, ARA&A, 27, 235
[148] Lauer T. R., 1985, ApJ, 292, 104
[149] Faber S. M. et al. 1997, AJ, 114, 1771
[150] Bender R., Surma P., Doebereiner S., Moellenhoff C., Madejsky R., 1989, A&A, 217, 35
[151] Davies R. L., Efstathiou G., Fall S. M., Illingworth G., Schechter P. L., 1983, ApJ, 266, 41
[152] Forbes D. A., Franx M., Illingworth G. D., Carollo C. M., 1996, ApJ, 467, 126
[153] van der Marel R. P., 1999, AJ, 117, 744
[154] Trentham N., Tully R. B., Verheijen M. A. W, 2001, MNRAS, 325, 1275
[155] Doublier V., Caulet A., Comte G.., 1999, A&AS, 138, 213
[156] Drinkwater M. J., Gregg M. D., 1998, MNRAS, 296, L15
[157] Phillipps S.,. Drinkwater M. J., Gregg M. D., Jones J. B., 2001, ApJ, 560, 201
[158] Freeman K. C., 1970, ApJ, 160, 811
[159] Binggeli B., Cameron L. M., 1991, A&A, 252, 27
[160] King I. R., 1966, AJ, 71, 64
[161] Harris W. E. et al., 1997, AJ, 114, 1030
[162] Gnedin O., Lahav O., Rees M. J., 2001 (astro-ph/0108034)
[163] van der Marel R. P., Gerssen J., Guhatakurta P., Peterson R. C., Gebhardt K., 2002, AJ, 124, 3255
[164] Gerssen J., van der Marel R. P., Gebhardt K., Guhatakurta P., Peterson R. C., Pryor C., 2002, AJ, 124, 3270
[165] Marín-French A., Aparicio A., 2003, ApJ, 585, 714
[166] Hodge P., 1994, in Munoz-Tunon C., Sanchez F., ed., The Formation and Evolution of Galaxies. Cambridge University Press, Cambridge, p. 1
[167] Feltzing S., Gilmore G., Wyse R. F. G., 1999, ApJ, 516, 17
[168] Wyse R. F. G., Gilmore G., Houdashelt M. L., Feltzing S., Hebb L., Gallagher J. S., Smecker-Hane T. A., 2002, New Astron., 7, 395
[169] Armandroff T. E., da Costa G., 1991, AJ, 101, 1329
[170] Bruzual A. G., Charlot S., 1993, ApJ, 405, 538
[171] Ferrini F., Poggianti B. M., 1993, ApJ, 410, 44
[172] Leiherer C. et al. 1996, PASP, 108, 996
[173] Fioc M., Rocca-Volmerange B., 1997, A&A, 326, 950
[174] Poggianti B. M., Barbaro G., 1997, A&A, 325, 1025
[175] Kodama T., Arimoto N., 1997, A&A, 320, 41
[176] Charlot S., Worthey G., Bressan A., 1996, ApJ, 457, 625
[177] Szokoly G. P., Subbarao M. U., Connolly A. J., Mobasher B., 1998, ApJ, 492, 452
[178] Thronson H. A., Greenhouse M. A., 1998, ApJ, 327, 671
[179] de Jong R. S., 1996, A&A, 313, 377
[180] Walker T. P., Steigman G., Kang H.-S., Schramm D. M., Olive K. M., 1991, ApJ, 376, 51
[181] Smith M. S., Kawano L. H., Malaney R. A., 1993, ApJS, 85, 219
[182] Songaila A., Wampler E. J., Cowie L. L., 1997, Nature, 385, 137
[183] O'Meara J. M., Tytler D., Kirkman D., Suzuki N., Prochaska J. X., Lubin D., Wolfe A. M., 2001, ApJ, 552, 718
[184] Ruhl J. E. et al., 2002 (astro-ph/0212229)
[185] Benoit A. et al., 2003, A&A, 399, L25
[186] Weinberg D., Miralda-Escudé J., Hernquist L., Katz N., 1997, ApJ, 490, 564
[187] Perlmutter S. et al., 1999, ApJ, 517, 565
[188] White S. D. M., Navarro J. F., Evrard A. E., Frenk C. S., 1993, Nature, 366, 429
[189] Evans N. W., Wilkinson M. I., 2000, MNRAS, 316, 929
[190] Trentham N., Moeller O., Ramirez-Ruiz E., 2001, MNRAS, 322, 658
[191] Press W. H., Schechter P., 1974, ApJ, 187, 425

[192] Efstathiou G., Bond J. R., White S. D. M, 1992, MNRAS, 258, 1p
[193] Wilkinson M. I., Evans N. W., 1999, MNRAS, 310, 645
[194] Kleyna J. T., Wilkinson M. I., Evans N. W., Gilmore G., 2001, ApJ, 563, L115
[195] Gerhard O. E., Spergel D. N., 1992, ApJ, 389, L9
[196] van den Bergh S., 1992, A&A, 264, 75
[197] Papovich C., Dickinson M., Ferguson H. C., 2001, ApJ, 559, 520
[198] Dickinson M., Papovich C., Ferguson H. C., Budavari T., 2003, ApJ, in press (astro-ph/0212242)
[199] Brinchmann J., Ellis R. S., 2000, ApJ, 536, L77
[200] Barlow T. A., Tytler D., 1998, AJ, 115, 1725
[201] Pettini M., Ellison S. L., Schaye J., Songaila A., Steidel C., Ferrara A., 2001, Ap&SSS, 277, 555
[202] Ellison S. L., Songaila A., Schaye J., Pettini M., 2000, AJ, 120, 1175
[203] Misawa T., Tytler D., Iye M., Storrie-Lombardi L. J., Suzuki N., Wolfe A. M., 2002, AJ, 123, 1847
[204] Telfer R. C., Kriss G. A., Zheng W., Davidsen A. F., Tytler D., 2002, ApJ, 579, 500
[205] Webb J. K., Carswell R. F., Lanzetta K. M., Ferlet R., Lemoine M., Vidal-Madjar A., Bowen D. V., 1997, Nature, 388, 250
[206] Lynden-Bell D., 1967, MNRAS, 136, 101
[207] Fulton E., Barnes J. E., 2001, Ap&SS, 2001, 276, 851
[208] http://www.ast.cam.ac.uk/~optics/cirpass/index.html
Mihos J. C., Dubinski J., Hernquist L., 1998, ApJ, 494, 183
[209] Dejonghe H., Habing J., 1993, IAU Symposium 153: Galactic Bulges. Kluwer Academic Publishers, Dordrecht
[210] Mihos J. C., Dubinski J., Hernquist L., 1998, ApJ, 494, 183
[211] Haehnelt M. G., Natarajan P., Rees, 1998, MNRAS, 300, 817
[212] Lacy M., Ridgway S., Trentham N., 2002, in Biretta J., Koekemoer A. M., Perlman E. S., O'Dea C. P., eds, Life Cycles of Radio Galaxies, New Astronomy Reviews, 46, 211
[213] Kukula M. J., Dunlop J. S., McLure R. J., Miller L., Percival W. J., Baum S. A., O'Dea C. P., 2001, MNRAS, 326, 1533
[214] Boyle B. J., Terlevich R. J., 1998, MNRAS, 293, L49
[215] Schweizer F., 1986, Science, 231, 227
[216] Gebhardt K. et al., 2001, AJ, 122, 2469
[217] Kormendy J., Bender R., M31 binary
[218] Komossa S., Burwitz V., Hasinger G., Predehl, P.; Kaastra, J. S.; Ikebe, Y., 2003, ApJ, 582, L15
[219] Gnedin O., 1999, BAAS, 65.04
[220] Metcalfe N., Shanks T., Campos A., McCracken H. J., Fong R., 2001, MNRAS, 323, 795
[221] Gardner J. P., Cowie L. L., Wainscoat R. J., 1993, ApJ, 415, L9
[222] Cowie L. L., Gardner J. P., Hu E. M., Songaila A., Hodapp K.-W., Wainscoat R. J., 1994, ApJ, 434, 114
[223] Huang J.-S., Cowie L. L., Gardner J. P., Hu E. M., Songaila A., Wainscoat R. J., 1997, ApJ, 476, 12
[224] Eggen O. J., Lynden-Bell D., Sandage A. R., 1962, ApJ, 136, 748
[225] White S. D. M, Kauffmann G., in Munoz-Tunon C., Sanchez F., eds., The Formation and Evolution of Galaxies. Cambridge University Press, Cambridge, p. 455
[226] Cole S., Lacey C. G., Baugh C. M., Frenk C. S., 2000, MNRAS, 319, 168
[227] Mathis H., Lemson G., Springel V., Kauffmann G., White S. D. M, Eldar A., Dekel A., 2002, MNRAS, 333, 739
[228] Efstathiou G., 2000, MNRAS, 317, 697
[A1] Chapman S. C., Blain A. W., Ivison R. J., Smail I. R., 2003, Nature, 422, 695
[A2] Boyle B. J. et al., MNRAS, 317, 1014
[A3] Budavari T. et al., 2003, ApJ, in press (astro-ph/0305603)
[A4] Erb D. K., Shapley A. E., Steidel C. C., Pettini M., Adelberger K. L., Hunt M. P., Moorwood A. F., Cuby J.-G., 2003, ApJ, in press (astro-ph/0303392)

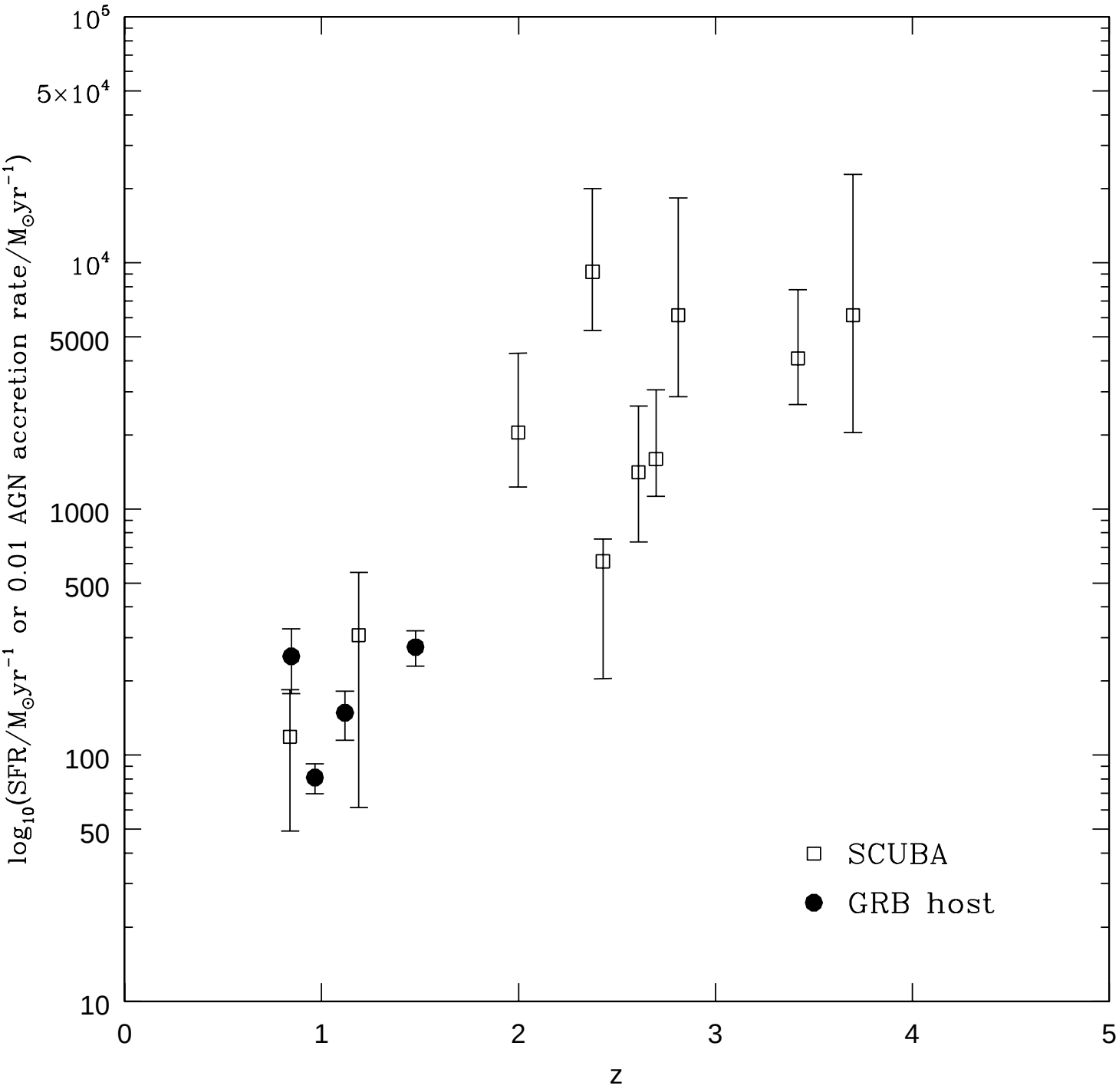
10^5
5×10^4
10^4
5000
1000
500
100
50
10
0
1
2
3
4
5
z
$\log_{10}(\mathrm{SFR}/\mathrm{M}_\odot\mathrm{yr}^{-1}$ or 0.01 AGN accretion rate/$\mathrm{M}_\odot\mathrm{yr}^{-1})$
SCUBA
GRB host